THESIS

GEOPHYSICAL CONSTRAINTS ON THE FLEXURAL SUBSIDENCE OF THE DENVER BASIN

Submitted by

Ayrat Abdullin

Department of Geosciences

In partial fulfillment of the requirements

For the Degree of Master of Science

Colorado State University

Fort Collins, Colorado

Fall 2012

Master's Committee:

Advisor: Dennis L. Harry

Sven Egenhoff
Michael Lefsky

ABSTRACT

GEOPHYSICAL CONSTRAINTS

ON THE FLEXURAL SUBSIDENCE OF THE DENVER BASIN

The Denver Basin is an asymmetric Laramide (Late Cretaceous through Eocene) foreland basin covering portions of eastern Colorado, northwestern Kansas, southwestern Nebraska, and southeastern Wyoming, USA. It is bordered on the west by the Rocky Mountain Front Range Uplift, a basement cored Laramide anticline bounded by thrust faults, and on the east by the Great Plains and stable North American craton. A ~400 mGal negative Bouguer gravity anomaly exists over the Denver Basin and Front Range Uplift, with its minimum located over the highest topography in the central part of the uplift, approximately 100 km west of the Denver Basin. This study examines three hypotheses concerning the isostatic state of the basin and adjacent Front Range Uplift. These hypotheses are that the modern shape of the basin is due to:

1) flexure of the lithosphere under the surface load of the current topography, or
2) flexure under a subsurface load beneath the Rocky Mountains, or
3) a combination of both surface and subsurface loads.

To test these hypotheses, spectral analysis and forward gravity modeling was conducted along three profiles located in the northern, central, and southern parts of the basin. Bouguer gravity power spectra along the profiles reveal 5 major density interfaces interpreted to represent the base of the lithosphere (at depths of 132 to 153 km), base of the crust (45-55 km), a mid-crustal boundary (about 20 km), the top of Precambrian basement (1-2 km), and a boundary between the Pierre Shale and Niobrara Formations within the pre-Laramide sedimentary section (-1-0 km). Flexural modeling shows that the shape of the basin can be fit with an elastic plate model having a line load of magnitude 2-5 x 10^{12} N/m and an elastic

thickness of the lithosphere of 58-80 km. The location of the load is 90-115 km west of the Bouguer gravity minimum on each profile. The gravity anomaly associated with flexural subsidence of the basin, assuming the layered density structure derived from the spectral analysis, is calculated to reach a minimum of -60 mGal, only 15 % of the observed Bouguer gravity anomaly. The magnitude of the load is less than the present topography weight of 3.63-4.65 x 10^{13} N/m, indicating that the weight of the Rocky Mountain Front Range is only partially compensated by flexural isostasy. Since seismic data indicate a lack of a pronounced crustal root, a buoyant subsurface load is required (hypothesis 3). Forward gravity models, supplemented with available well and seismic refraction data, are developed to test four end-member hypotheses as to the location of the buoyant subsurface load. We consider in turn that the load lies entirely within the: (1) asthenosphere, (2) shallow lithosphere mantle, (3) lower crust, or (4) upper crust. The models show that the subsurface load is unlikely to lie entirely within any of the depth intervals investigated. The study indicates that the buoyant subsurface load is partitioned in some combination between low-density crust and/or low-density lithospheric and/or asthenospheric mantle. In all of the gravity models, the crust thickens abruptly at the boundary between the Rocky Mountains and Great Plains, from about 48 km beneath the Denver Basin to about 53 km beneath the Front Range Uplift.

ACKNOWLEDGEMENTS

This work would not have been possible without so many people.

I would like to express my sincere gratitude to Dr. Dennis Harry, my advisor, for invaluable supervision of this research. His technical input, critical reviews, enthusiasm, and overall experience were vital to the completion of this project. I would also like to thank Drs. Sven Egenhoff and Michael Lefsky from my master's committee for their guidance and comments on this project. To the professors at Colorado State University who have all been friends as well as teachers, thank you. To the past and present graduate students in the Department of Geosciences, thank you.

Funding for this research was provided by the Stone-Hollberg scholarship from the Rocky Mountain Association of Geologists (RMAG) Foundation. I would also like to thank the PACE committee members of the European Association of the Geoscientists and Engineers (EAGE) for providing a travel grant to the 74th EAGE Conference & Exhibition, which led to invaluable feedback and knowledge from the scientific community on my research project.

Finally, I would like to thank my family and my roommate Ildus Mingazetdinov for encouragement and unwavering support during the production of this thesis.

Oh, almost forgot… Thanks God!

DEDICATION

To my Mom,
for the love and support
that she has always given me,
and the desire to see her son
finish his education.

TABLE OF CONTENTS

LIST OF TABLES

LIST OF FIGURES

CHAPTER 1

INTRODUCTION

1.1 Background

The Denver Basin is an asymmetrical Laramide foreland basin covering about 155,000 km^2 (60,000 square miles) in portions of eastern Colorado, northwestern Kansas, southwestern Nebraska, and southeastern Wyoming (Copland, 1984; Higley et al., 2002). The Denver Basin is one of the largest structural basins in the area east of the Rocky Mountains. The Denver basin has abundant natural resources, including oil and gas, coal, sand and gravel, and groundwater reservoirs in its upper formations (Fishman, 2005). The four principal aquifers within the Denver Basin in eastern Colorado represent a tremendous groundwater resource. This system of multi-layered sandstones and siltstones is estimated to contain over 200 million acre-feet of recoverable groundwater (Topper and Raynolds, 2007).

The Denver basin formed as a foreland basin during the Laramide Orogeny in late Cretaceous and early Tertiary time (Dickinson, 1986). During Middle Maestrichtian time, the beginning of the Laramide Orogeny in Colorado, a proto-basin had begun to take shape and by the Middle Eocene (the end of the Laramide Orogeny) the basin had become a closed structural feature. The basin continued to subside until the end of the Tertiary, by which time the Laramide topography had been eroded (Scott, 1975; Christiansen and Yeats, 1992; Weimer and Sonnenberg, 1996). Since then the entire region has been uplifted, producing the modern Rocky Mountain topography (Tainter, 1982; McMillan et al., 2006; Karlstrom et al., 2011).

1.2 Goals, Objectives, and Methodology

The processes controlling the tectonic subsidence of the Denver Basin and high elevation of the basin and adjacent Rocky Mountain Front Range are poorly understood. The main hypothesis of this study is that the flexural shape of the modern Denver basin is maintained by a negatively buoyant load associated with the Front Range Uplift. The thesis tests this hypothesis by examining the isostatic balance of the Rocky Mountain Front Range Uplift and Denver Basin tectonic system. The goals are to determine whether the weight of the Front Range Uplift topography is sufficient to account for the flexural subsidence of the Denver Basin, whether the Front Range topography is fully supported by flexural isostasy, and, if not, the magnitude and depth of the subsurface load required to isostatically balance the system. The results of the research place better constraints on the geologic and tectonic conditions in which the basin and Front Range Uplift formed than are currently recognized. The main geophysical data used is a regional gravity survey, supplemented with relatively sparse well and deep seismic data. The Bouguer gravity power spectra are used to estimate an average layered density structure for the lithosphere in the region. Flexural modeling is then used to estimate the flexural rigidity and the magnitude and position of the associated loads required to produce the modern flexural shape of the Denver Basin. Finally, forward gravity modeling is used to build three geologic cross-sections constructed perpendicular to the strike of the basin axis to examine how the subsurface component of the load is distributed.

The research has importance on regional, continental, and global scale tectonic studies. On the regional scale, understanding the flexural evolution of the Denver Basin provides a tectonic framework to develop better models for oil and gas exploration and production. Since depositional patterns in the basin are a response to differential uplift and subsidence, understanding tectonic forces driving subsidence in the Denver basin can help quantify depositional patterns and subsurface distribution of bedrock aquifers. On a continental scale,

this project sheds light on central North American tectonics. In particular, the reasons for the high elevation and relatively shallow depth of the Denver Basin and development of the Laramide structures of the Rocky Mountains under the influence of the subsurface loading. Finally, this study improves understanding of how foreland basins in large scale orogenic systems respond to tectonic loading, and how such loads are emplaced through space and time.

The key finding of this research is that subsidence in the Denver Basin is insufficient to flexurally support the weight of the Front Range Uplift. The crustal root beneath the Rocky Mountains is similarly insufficient to provide the remaining buoyancy required for isostatic support. These results suggest a complex density structure developed within the mantle beneath the Southern Rocky Mountain Front Range region since Middle Miocene. The buoyancy is at least partly and, perhaps, entirely, located within the sublithospheric mantle.

1.3 Organization of Thesis

The data collection and processing, analysis and modeling, and project conclusions explained in this thesis are organized into a scientific paper to be submitted to a professional journal (AGU Journal of Geophysical Research), which is presented in Chapter 2. Chapter 3 presents some recommendations to help future research in the study area or similar foreland basins systems elsewhere.

REFERENCES

Christiansen, R. L., and R. S. Yeats (1992), Chapter 7. Post-Laramide geology of the U.S. Cordilleran region, in *The Cordilleran Orogen, Conterminous U.S., The geology of North America, G-3*, edited by B. C. Burchfiel, P. W. Lipman, and M. L. Zoback, pp. 261–406, Geological Society of America, United States.

Copland, J. R. (1984), Laramide structural deformation at the interface between the Laramie Range and the Denver-Julesburg Basin, Southeastern Wyoming, M.S. thesis, Dep. of Geol. and Geophys., Univ. of Wyoming, Laramie, Wyoming, USA.

Dickinson, M. (1986), A search for intrasedimentary aeromagnetic anomalies over a known oil field in the Denver Basin, M.S. thesis, Dep. of Geol. and Geophys., Colorado School of Mines, Golden, Colorado, USA.

Fishman, N. S. (2005), *Energy Resource Studies, Northern Front Range, Colorado, Professional Paper 1698*, USGS, Reston, Virginia.

Higley, D. K., R. R. Charpentier, T. A. Cook, T. R. Klett, R. M. Pollastro, and J. W. Schmoker (2002), Executive summary – 2002; Assessment of undiscovered oil and gas in the Denver Basin province, Colorado, Kansas, Nebraska, South Dakota, and Wyoming, *U.S. Geological Survey Digital Data Series DDS–69–P*.

Karlstrom, K. E., and CREST Working Group (2011), Mantle-driven dynamic uplift of the Rocky Mountains and Colorado Plateau and its surface response; toward a unified hypothesis, *Lithosphere*, *4*(1), 3-22, doi:10.1130/L150.1.

McMillan, M. E., P. L. Heller, and S. L. Wing (2006), History and causes of post-Laramide relief in the Rocky Mountain orogenic plateau, *Geological Society of America Bulletin*, *118*, 393–405, doi: 10.1130/B25712.1.

Scott, G. R. (1975), Cenozoic surfaces and deposits in the southern Rocky Mountains, *Geological Society of America Memoir 144*, 227–248.

Tainter, P. A. (1982), An effective exploration strategy: stratigraphic and paleostructural controls on hydrocarbon migration in the Denver Basin, *AAPG Bulletin*, *66*(5), 635-636.

Topper, R., and B. Raynolds (2007), *Citizen's guide to Denver Basin groundwater*, Colorado Foundation for Water Education, Denver, Colorado.

Weimer, R. J. and S. A. Sonnenberg (1996), Guide to the petroleum geology and Laramide orogeny, Denver Basin and Front Range, Colorado, *Colorado Geological Survey Bulletin, 51*.

CHAPTER 2

GEOPHYSICAL CONSTRAINTS

ON THE FLEXURAL SUBSIDENCE OF THE DENVER BASIN

1. Introduction

The Denver Basin (Fig. 1) is an asymmetric Laramide foreland basin covering about 155,000 km^2 (60,000 square miles) in portions of eastern Colorado, northwestern Kansas, southwestern Nebraska, and southeastern Wyoming (Copland, 1984; Higley et al., 2002). The sedimentary section reaches a maximum of approximately 4,200 m next to the Rocky Mountain Front Range near Denver, Colorado (Kinney, 1967); the Denver Basin fill itself reaches about 1,000 m (Raynolds, 2002). Previous studies have shown that the weights of these and Great Plains sediments, and the basement rocks of the nearby mountain ranges are too heavy to explain the relatively shallow depth of the Denver Basin (Angevine and Flanagan, 1987; Babits, 1987). The basin should contain more than 6 km of sediment according to isostatic considerations (Angevine and Flanagan, 1987). Hence, the Denver Basin cannot be explained only by flexural isostatic compensation of the lithosphere under the current topography load, and the weight of the Rocky Mountain uplifts must be partially supported by a subsurface load (in addition to flexure). This study is devoted to determine where the subsurface load might be located and how large it is. This project combines geodynamic modeling of plate flexure with analysis of topography and the regional gravity field in the Denver Basin and adjacent mountain regions. The research constrains the magnitude and location of the associated loads.

In this paper, gravity data is used to develop a lithosphere-scale subsurface density model of the Denver Basin and adjacent areas of the High Plains and Rocky Mountain Front Range. Three gravity profiles are located in the northern, central and southern parts of the Denver

Basin (Fig. 1), traversing the Front Range Uplift, the basin, and western part of the Great Plains. The profiles are oriented perpendicular to the strike of the regional Bouguer gravity minimum. Bouguer gravity power spectra from each profile are used to determine an approximate average layered density model of the lithosphere across each profile. Flexural modeling is then used to estimate the flexural rigidity and the magnitude and position of the total load required to produce the modern flexural shape of the Denver Basin. Forward gravity models across the three geologic cross-sections are constructed perpendicular to the strike of the basin axis to examine how the subsurface component of the load is distributed.

2. Geological Setting

The Denver Basin is located immediately east of the Front Range uplift of the Southern Rocky Mountains (Fig. 1). The basin does not have a well-defined eastern boundary (Hemborg, 1996; Weimer and Sonnenberg, 1996). It is bounded on the west by the uplifted Front Range of the Rocky Mountains, on the north by the Hartville uplift, Black Hills, and Chadron-Cambridge Arch, on the east by a gentle onlapping relationship onto the stable mid-continent craton, and on the south by the Apishapa Arch separating it from the Raton Basin (Raynolds, 2002).

Prior to Late Cretaceous, the area now occupied by the Denver Basin and adjacent Rocky Mountain and Great Plains regions consisted of a flat, stable platform underlying the shallow Cretaceous Western Interior Sea (Mallory, 1972; Tweto, 1975). Subsidence of this platform and extensive marine deposition during late Early Cretaceous and Late Cretaceous is marked by deposition of the Dakota and Benton Groups, Niobrara Formation, Pierre Shale, Fox Hills and Laramie Formations (Figs. 2, 3). The spatial distribution and thickness of these formations have been attributed to flexure of the North American craton by loading by the Sevier thrust belt about 700 km further west (Cross and Pilger, 1978; Jordan, 1981). The

Sevier thrust belt has been attributed to shallow low-angle subduction of the Farallon plate (Cross and Pilger, 1978; Bird, 1984). Up to 3.2 km of the Pre-Sevier and Sevier sediment contained in the Denver basin area was deposited during the Cambrian-Late Cretaceous period before it became a distinct foreland basin (Babits, 1987).

3. Tectonic History

Two distinct periods of deformation resulted in the current geometry of the Denver Basin and adjacent basement uplifts (Curtis, 1975) (Figure 4). The first major period of deformation is the Laramide orogeny of Late Cretaceous-Eocene age (Tweto, 1975; Gries, 1983; Steidtmann and Middleton, 1991). Once Laramide deformation started within the central Rocky Mountain region, the whole foreland province was fragmented into separate local basins. They were sedimentologically isolated and detached by developing basement-cored uplifts, which functioned as local sources of orogenic clastic sediments (Dickinson et al., 1988). The entire Laramide province was then occupied by diverse nonmarine settings, and local facies sequences were restricted in lateral extent to separate basins bounded by adjacent uplifts. Ultimate regression of the Late Cretaceous Seaway from the western-central region occurred during the beginning of the Laramide orogeny (Tweto, 1980; Bird, 1984).

Laramide tectonic structures are characterized by asymmetric basement-cored folds with wavelengths up to several hundred kilometers, and often bounded by reverse faults (Gries, 1983; Lowell, 1983). The Front Range uplift, a Laramide anticline bordering the west side of the Denver Basin, has been uplifted compared to the Great Plains since the onset of the Laramide orogeny (Raynolds et al., 2007). This uplift, which has uncovered Precambrian rocks along its length, was initiated partly by horizontal basement shortening on a series of thrust faults along the sides of the uplift (Johnson, 1985; Karlstrom et al., 2005) (Figure 5). In spite of the large size of the Front Range uplift and the Denver basin as structural features,

only a minor part of the basin contains Laramide-age strata (Arapahoe and Denver Formations and Dawson Arkose, Fig. 3) nowadays: the sediments occur mostly in the basin center and extend eastward no more than 100 km from the mountain front (McDonald, 1972; Raynolds, 2002). The overall thickness of these nonmarine clastic sedimentary rocks is more than 800 m (Raynolds et al., 2007). Maastrichtian beginning of Laramide deformation was roughly synchronous all over the Laramide province, but the cessation of Laramide deformation progressed diachronously from north to south in Early-Late Eocene time (Dickinson et al., 1988).

In the Front Range, Denver Basin and Great Plains the Middle to Late Eocene, following the Laramide orogeny, was a period of tectonic quiescence and erosion which greatly destroyed Laramide relief (Scott, 1975; Christiansen and Yeats, 1992; Weimer and Sonnenberg, 1996). As a result, an extensive erosion surface was formed across the regions currently occupied by mountains and plains alike (Scott, 1975; Epis and Chapin, 1975; Bradley, 1987). This erosion surface is preserved below volcaniclastic sedimentary rocks of Oligocene and early Miocene age (Morse, 1985). In the Denver Basin the Wall Mountain ignimbrite dated at 36.7 Ma (McIntosh and Chapin, 1994) lies unconformably atop the Dawson Formation (Epis and Chapin, 1974; Trimble, 1980) and is generally considered to provide a maximum age for cessation of basin subsidence. The ignimbrite is associated with tectonism occurring in the eastern edge of the emerging Basin and Range province to the west (Trimble, 1980).

Since the late Miocene (ca. 10 Ma) the western Great Plains became an area of downcutting and erosion (Stanley and Wayne, 1972) removing 2-3 km (Trimble, 1980) of the upper Tertiary fill from the Denver basin. This downcutting has been interpreted to result from regional epeirogenic uplift of the Rocky Mountain region (McMillan et al., 2006; Karlstrom et al., 2011). The current relative relief of the Front Range has been argued to be a

function of differential erosion, not uplift (Raynolds et al., 2007). Alternatively, Quaternary normal faults in the basin (Tweto, 1979a) imply that crustal extension and differential uplift of mountains and plains has been ongoing since the Late Cenozoic, leading to 1.5 to 3 km (based on the correlation of deposits on the Eocene erosion surface, Epis and Chapin, 1975) of regional uplift in the southern Rocky Mountains and western Great Plains (DeCelles et al., 1991; Hoy and Ridgway, 1997). Suggested mechanisms that possibly could cause surface uplift of the Rocky Mountain orogenic plateau include isostatic and dynamic processes associated with mantle flow, mid-crustal flow, anomalous changes in composition or thermal regime of the crust and mantle, or rebound driven by the foundering of the Farallon slab (Dickinson and Snyder, 1979; Morgan and Swanberg, 1985; Severinghaus and Atwater, 1990; Humphreys and Dueker, 1994; Humphreys, 1995; Spencer, 1996; Burgess et al., 1997; McQuarrie and Chase, 2000; Heller et al., 2003; McMillan et al., 2006; Karlstrom et al., 2011).

4. Lithospheric flexure and load partitioning in foreland basins

4.1 Flexural subsidence in foreland basins

Numerous studies (Walcott, 1970; Haxby et al., 1976; Beaumont, 1978, 1981; Jordan, 1981; Watts et al., 1982; Karner and Watts, 1983; Garner and Turcotte, 1984; Babits, 1987; Egan, 1992; Macario et al., 1995; McKenzie and Fairhead, 1997; Stewart and Watts, 1997; Burov et al., 1998; Petit and Ebinger, 2000; Simons et al., 2000; Banks et al., 2001) have tested the response of the continental lithosphere to applied tectonic loads such as those created by orogenic processes. These studies show that the continental lithosphere can be effectively modeled as an elastic plate. In this model, long wavelength (>50 km) mountain topography is compensated regionally by downward flexure of the lithosphere, with the

flexural deformation extending well beyond the leading edge of the uplift. This creates a flexural foreland basin adjacent to the range and a more distal flexural uplift.

4.2 Partitioning of the load into subsurface and surface loads

Previous studies show that in addition to the surface loads of thrust sheets, basement uplifts, and sedimentary basin fill, positively and/or negatively buoyant subsurface loads may also play an important role in the development of mountain-foreland basin systems (Karner and Watts, 1983; Royden and Karner, 1984; Forsyth, 1985; Angevine and Flanagan, 1987; Babits, 1987; Stewart and Watts, 1997; McKenzie, 2003). Subsurface loads can be the governing factor on the deflection of the lithosphere and, as such, may be considered as the primary load in such orogenic systems (Karner and Watts, 1983). In some instances, subsurface loads may be the major control on both foreland basin formation and general crustal structure. The emplacement of large subsurface loads characterizes the primary event in the Alps and Appalachians, whereas in the Himalayas the emplacement of the surface load is the primary event (Karner and Watts, 1983).

5. Subsurface Density Structure beneath the Denver Basin and Front Range Uplift

A large long-wavelength negative isostatic gravity anomaly is present over the Denver Basin, the Great Plains, and the southern Rocky Mountains after correcting for the isostatic effects of the sediment fill and the basement uplifts (Reinke, 1991). Crustal corrections applied to North American Bouguer gravity data infer major (0.06 to -0.08 g/cc) upper mantle density anomalies of thermal and compositional origin (Mooney and Kaban, 2010). Based on the gravity data, Angevine and Flanagan (1987) showed that the western Great Plains are underlain by a positively buoyant subsurface load that explains the high regional elevations and the shallowness of the Denver basin. Gravity and flexure models (Babits, 1987) show

that a buoyant subsurface load balancing 25-70% of the surface load is necessary to satisfy both the large negative Bouguer gravity anomalies and the Precambrian basement depth in the Denver basin. The estimated mass deficit is maximum beneath the Rocky Mountains and decreases to the north and to the east (Reinke, 1991).

The origin of the subsurface load has been suggested to include the following possibilities:

1) Low-density deep upper mantle (asthenosphere)

1.1) Lithospheric thinning

Angevine and Flanagan (1987) argued that the subsurface load may have resulted from thinning of the lithospheric mantle, which often accompanies or precedes crustal extension. Bird's (1988, 1998) model of subcrustal shearing predicts a thin mantle lithosphere across the Laramide foreland which thickens eastward due to underplating of sheared mantle lithosphere. Lithospheric thinning can explain a buoyant subsurface load due to hot light asthenospheric material substituting denser mantle lithosphere (Reinke, 1991). Eaton (1987) argued that this may have coincided with regional uplift and lithospheric extension throughout the western portion of the basin which began in Miocene time. There are Miocene-age normal faults in much of north central Colorado and south central Wyoming (Izett, 1975). Normal faulting related to the Rio Grande Rift can be mapped out along the ridge of the Rocky Mountains into northern Colorado with diminishing effect as it reaches the Wyoming border (Chapin and Cather, 1994; Naeser et al., 2002; Buffler, 2003). Further evidence of lithospheric thinning consists of delay times for P-wave arrivals (Cleary and Hales, 1966; Olsen et al., 1979; Allenby and Schnetzler, 1983; Schmandt and Humphreys, 2010) and upper mantle electrical conductivities (Porath, 1971) over the basin area, and high heat flow in Northern Colorado (Lachenbruch and Sass, 1977; Decker et al., 1980, 1988). These facts agree with the northward propagation of the Rio Grande Rift over time (Tweto, 1979a; Chapin and Cather, 1994).

1.2) Thermal sources

Dueker et al. (2001) imaged low-velocity, upper mantle anomalies in the Rocky Mountain-Colorado Plateau region, which are characterized by small P-wave-velocity anomalies (-2% perturbations) that extend to 200–250 km depth. Schmandt and Humphreys (2010) suggested that these velocity anomalies could have a thermal origin associated with asthenospheric convection.

Karlstrom et al. (2005) associate the source of the increased mantle heat flow through time with upwelling asthenosphere (Moucha et al., 2009) related to sinking of the lower lithosphere isotherms (Schott et al., 2000) or Neogene development of upper mantle small-scale free convection (Korenaga and Jordan, 2003; Karlstrom et al., 2008; Schmandt and Humphreys, 2010; Van Wijk et al., 2010).

1.3) Compositional sources

The eastern U.S. mantle is so cold that the average elevation should be lower than it is. A compositionally induced density decrease over a depth interval of 50–250 km is suggested by Goes and van der Lee (2002) to balance the topographic effect of the thermally implied density increase for the North American craton.

The upper mantle in the western U.S. was likely altered by a combination of Cenozoic events, including hydration above the Farallon slab (Bird, 1988; Humphreys et al., 2003) and partial melting and intrusion during the ignimbrite eruption (Humphreys, 1995) and Neogene magmatism (Karlstrom et al., 2002).

1.4) Partial melt

Small-scale velocity anomalies imaged with P- and S-wave tomography indicate that locally 1% melt could be present under the southwestern edge of the Colorado Plateau and parts of the Rio Grande Rift (Goes and van der Lee, 2002).

2) Low-density shallow upper mantle

Seismic tomographic data along the CD-ROM transect from Wyoming to New Mexico show that the upper mantle, down to depths of more than 200 km, has a number of dipping velocity anomalies that project up to overlying Proterozoic crustal boundaries (Karlstrom et al., 2002).

Large P- and S-wave negative velocity anomalies up to -3% are centered beneath the southern Rocky Mountains (Dueker et al., 2001; Goes and van der Lee, 2002; Schmandt and Humphreys, 2010). Goes and van der Lee (2002) inferred from these velocity anomalies that temperatures in the cratonic mantle at 50–100 km beneath the tectonic western part of North America are on average 500°C higher than under the stable eastern part of the continent. They calculated the combined isostatic effect of these anomalies, which results in a domal shape of high topography with 1–2 km of predicted relief between the Rocky Mountains and the central Great Plains. This feature agrees with indications of extensive subsurface upward directed loading according to gravity modeling (Angevine and Flanagan, 1987), crustal thickness estimates interpreted from P-wave velocities (Sheehan et al., 1995), and flexural modeling of the southern flanks of the Rio Grande Rift (Roy et al., 1999).

The model by Keller et al. (2005) implies that the Moho boundary under the Rocky Mountains has been dynamically restructured by mafic magmatism such that its existing complexity (10-km-scale topography, and variations in lower crustal and upper mantle velocity) is a result of episodic addition of basaltic magmas due to partial melting of the asthenosphere, a process that reduces density of the continental lithospheric mantle (Karlstrom et al., 2005).

3) Low-density crust and crustal thickening

Bird (1984) suggested crustal thickening as an explanation for the buoyant subsurface load. It may be caused by two mechanisms: intrusion or horizontal transport of lower crustal

material, because of shear at the base of the crust (Bird, 1984). Tertiary volcanism is not widespread over the study area, casting doubt on crustal intrusion as a cause of much uplift. A horizontal transport mechanism implies at least a Laramide age for the uplift since there has not been any post-Laramide compression in the region. The mass transfer associated with mountain orogeny should be seismically detectable by differences in crustal velocities and thicknesses (Karner and Watts, 1983). The correlation between the age and thickness of the lithosphere across the Rocky Mountain Foreland suggests the Laramide Orogeny appears to not have altered the structure of the lower crust and upper mantle lithosphere (Keller et al., 1998; Snelson et al., 1998). Regional maps of crustal thickness estimates taken from seismic refraction and attribute analyses of seismic waves generated by distant earthquakes show a relatively planar Moho across the Rocky Mountain front (Snelson et al., 1998; Dueker et al., 2001; Li et al., 2002), despite 5-10 km of structural relief on the top of the Precambrian basement (Keefer and Love, 1963). Karlstrom et al. (2002) argued that crustal thickness variations across the Laramide province are closely related to the tectonic structure created during the Archean and Early Proterozoic rather than the Laramide orogeny. The thick crust beneath the Southern Rocky Mountains was mainly formed before 1.4 Ga, was eroded by about 10 km before the beginning of the Phanerozoic, and was mechanically thickened during the Laramide orogeny (Keller et al., 2005).

Regardless of the timing in which crust and mantle modification occurred, it is clear that the thickness of the crust in the Southern Rocky Mountains is not sufficient to isostatically support present regional high elevations (>3 km on average) (Sheehan et al., 1995; Lerner-Lam et al., 1998; Gilbert and Sheehan, 2004; Karlstrom et al., 2011). There is a possibility that density variations in the crust could be part of the subsurface load. Li et al. (2002) argued for shallow isostatic compensation of the Southern Rocky Mountains based on Rayleigh wave tomography data and found anomalously low-velocity crust in Central Colorado.

Gravity modeling implies that granite batholiths alone are not enough to account for the observed gravity field (McCoy et al., 2005). Hence, additional buoyancy from the upper mantle may provide the required support for the high topography (Sheehan et al., 1995; Gilbert, 2012).

6. Data Collection and Processing

Three 600-km-long Bouguer gravity profiles were constructed in the northern, central, and southern parts of the Denver Basin, transecting the Rocky Mountain Front Range, the basin, and the Western Great Plains (Fig. 1). The majority of gravity data was obtained from the PACES (Pan American Center for Earth and Environmental Studies) website (http://research.utep.edu/paces/). Only data lying within 10 km of the projected profiles were used. An additional approximately 500 gravity stations were collected to fill in areas of sparse data on the northern and central profiles, achieving 1-2 km average station spacing.

The newly collected gravity data were processed using the spreadsheet developed by Holom and Oldow (2007). Sea level was used as an elevation datum, and a density of 2.67 g/cc was used in Bouguer corrections. Instrument drift, Earth tide, instrument height, Free Air, atmospheric, Bouguer spherical cap, and terrain corrections were applied. The Bouguer gravity data were then integrated with the original PACES data to construct the profiles used in this thesis (Fig. 6).

7. Bouguer Power Spectra Analysis

A layered density model of the lithosphere can be determined from the slope of the logarithmic Bouguer gravity power spectra. Linear segments of the logarithmic power spectrum correspond to subsurface interfaces between layers of different density. The depth of each interface is given by one half of the slope of the appropriate segment of the power

spectrum, with steeper slopes corresponding to deeper interfaces (Banks et al., 1977; Karner and Watts, 1983).

The gravity data for each profile were resampled to a uniform 1 km interval using spline interpolation, because the spectral analysis requires a uniformly sampled data series. A 20% cosine taper was applied to the ends of the data series, and the Fast Fourier Transform was used to calculate the periodogram. The amplitude spectrum is estimated by calculating an averaging of the square of the periodogram within a moving window. Window lengths of 2-12 samples were tested, with 4 (north profile) and 6 (central and south) sample windows chosen as an optimal compromise between an overly smoothed spectrum and a spectrum with high variance (Bloomfield, 2000).

The Bouguer gravity spectra for the three profiles show 5-6 well-resolved linear segments, representing different interfaces at average depths for all profiles of 140, 45, 20, 8 and 1.5 km (Fig. 7). These are interpreted to represent the base of the lithosphere, at average depths on each individual profile of 132 to 153 km, base of the crust (45-55 km), mid-crustal boundary (about 20 km), average Precambrian basement depth (1-2 km), and boundary between Pierre Shale and Niobrara Formations (-1-0 km). The estimated thickness of the lithosphere is greater along the northern (153 km) and southern (144 km) profiles, than along the central profile (132 km). Precambrian basement is deeper along the central profile (2.1 km), than along the south one (0.7 km).

8. Flexural Modeling

8.1 Flexural fit to Bouguer gravity and Denver Basin subsidence

Flexural deformation of the lithosphere within the Denver Basin was modeled as the two-dimensional deflection of an infinite elastic plate (representing the lithosphere) overlying an

incompressible fluid (representing the asthenosphere). The equation governing flexure of an elastic plate is (Turcotte and Schubert, 2002):

$$w = \frac{V_0 \alpha^3}{4D} e^{-x/\alpha} cos\frac{x}{\alpha} \quad \text{and} \quad \alpha = \left[\frac{4D}{(\rho_m - \rho_w)g}\right]^{1/4}$$

where w is the plate deflection, V_0 is the magnitude of the applied line load, α is the flexural parameter, D is the flexural rigidity or stiffness of the plate, x is the position of the load, ρ_m is the mantle lithosphere density, ρ_w is the water (fluid) density, and g is the acceleration of gravity. Following Turcotte and Schubert (2002), a Young's modulus of 10^{11} Pa and Poisson's ratio of 0.25 were assumed. Flexural rigidity and the line load magnitude and location are free parameters that were iteratively modified until a satisfactory fit between observed and calculated basement deflection or Bouguer gravity was obtained, as described below.

The Bouguer gravity anomaly produced by flexure was calculated using Parker's (1972) method, assuming a simple layered density structure for the crust. The depths to the density interfaces used in calculating the theoretical gravity curves were taken from the Bouguer gravity power spectra analysis. The average densities of each layer were chosen based on the velocities derived from regional seismic survey data (Table 2, Figure 1). Only interfaces well-resolved by the spectral analysis with relatively large density contrasts were used in the modeling.

The flexural models first attempted to fit that portion of the Bouguer gravity anomaly that is the result of flexural subsidence in the basin. The positive anomaly dominating the Bouguer gravity field west of the gravity minimum was not modeled as a flexural feature. The flexural models that best fit the Bouguer gravity field in the Denver Basin have elastic thicknesses (T_e) ranging from 128-162 km, loads of magnitude 4-5 x 10^{13} N/m, and loads positioned 70-125 km west of the Denver Basin, within the Front Range Uplift and close to

the location of the Bouguer gravity minimum (Table 3). The T_e values of 133 and 128 km for the north and central profiles are smaller than 162 km for the south profile. There is a general trend of increasing load magnitude from north to south: from 4 x 10^{13} N/m on the northern profile to 5 x 10^{13} N/m on the southern profile. The modeled deflection of the crust is 8-10 km, which is about twice the observed deflection along the axis of the Denver Basin.

A second set of flexural models attempted to fit the shape of the Precambrian basement in the Denver basin (Hemborg, 1996); that is, these models attempt to fit the shape of the basin rather than the Bouguer gravity field. The calculated elastic thicknesses for the central and south profile are similar (58-60 km); the north profile has a bigger T_e = 80 km (Table 3). The load is similar for the north and central profile (4-5 x 10^{12} N/m), but it's smaller for the south profile (2 x 10^{12} N/m). The load position for the central profile (42 km) shifts to the west compared to the north (86 km) and south (182 km) profiles. The flexural models that best fit the basement subsidence pattern produce gravity anomalies of no larger than 60 mGal and show that flexural subsidence of the Denver Basin is not enough to produce the observed gravity field (Fig. 8).

8.2 Load estimation

Assuming the average upper crust density of 2.761 g/cc calculated using the velocity model by Rumpfhuber and Keller (2009) and velocity to density conversion equation (1) in Brocher (2005), the weight of the current topography across the Front Range Uplift to the west of the Denver Basin axis (a region no more than 600 km wide) is estimated to range from 3.63-4.65 x 10^{13} N/m for the three profiles. This is an order of magnitude larger than the loads required to produce the flexural shape of the basin. Thus, flexural isostasy cannot provide the sole support for the present Rocky Mountain topography. There must be a

subsurface buoyant load, or mass deficit, under the area helping to compensate the mountain range topography.

9. Forward Gravity Modeling

A series of forward gravity models were constructed to examine possible alternatives for placement of the subsurface load beneath the Front Range Uplift. The *GM-SYS*™ gravity modeling software (Geosoft, Inc.) was used for forward gravity modeling. The average layered density structure determined from the power spectral analysis was used as a starting model for each of the three profiles. The models were then modified considering crustal thickness variations and depth to basement constrained by well and seismic data. Because the focus of the modeling was on the deep density structure, no attempt was made to model the short-wavelength variations in the gravity field associated with relatively shallow structures. Instead, the models seek to fit the long-wavelength Bouguer gravity low associated with flexure in the basin and large-scale subsurface density variations beneath the mountains. The Precambrian basement faults and lithologic changes within the crystalline rocks of the Front Range Uplift were not explicitly included in the models and are likely causes of the short-wavelength gravity variations.

The subsurface density structure obtained from forward gravity modeling is shown in Figures 10-13. The geologic units exposed at the surface were determined from the geologic map of Colorado (Tweto, 1979b). Depth to Precambrian Basement was constrained using well data (German, 1982; cogcc.state.co.us: Table A1) and Precambrian basement maps for Colorado, Kansas, and Nebraska (Jewett and Merriam, 1959; Watkins, 1964; Hemborg, 1996). The depth to the crust-mantle boundary was constrained by regional seismic refraction surveys (Keller et al., 1998), receiver functions (Sheehan et al., 1995), and recent data from the EarthScope project (Gilbert, 2012). The crust-mantle boundary was assumed to maintain

the similar shape as the Precambrian basement in the Denver basin part of the profiles. The bottom of the model was taken to be the 410 km deep seismic discontinuity. The seismic and well data place strong constraints on the sedimentary section (formation tops) and basement depth in the Denver basin, and the depth of the crust-mantle boundary along the length of the profiles. The least well-constrained part of the models is the structure of the mid-crustal boundary.

The initial densities used in the models were based on density log data for sedimentary units (cogcc.state.co.us: Table A1) and were derived from seismic velocities for the crystalline crust and mantle (Rumpfhuber and Keller, 2009) using Brocher's (2005) equation. The density is taken to be 3.28 g/cc in the mantle, 2.968 g/cc in the lower crust, and 2.761 g/cc in the upper crust. Mesozoic and Paleozoic sedimentary units older than Pierre Shale are grouped together in the gravity models as "MzPz" units (Figure 5). The densities for sedimentary units are: MzPz – 2.65 g/cc, Pierre Shale – 2.73 g/cc, Laramie Formation – 2.3 g/cc, Fox Hills Sandstone – 2.3 g/cc, Tertiary units – 2.3 g/cc, and Quaternary deposits – 2 g/cc (Figures 2, 5).

Different families of models were developed to assess different scenarios for the depth of the mass deficit. These include models in which the mass deficiency is considered to lie entirely within the: (1) asthenosphere, (2) lithosphere mantle, (3) lower crust, (4) upper crust. The four families of models have the same eastern reference point at 107°W longitude (0 km), model bottom (410 km deep), asthenosphere-lithosphere mantle boundary (100 km deep), crustal thickness variations, basement flexure of the Denver Basin, and sedimentary unit thicknesses. The boundaries between density domains within the lithosphere mantle and crust (upper and lower) are modeled as vertical interfaces for simplicity and were spatially varied during modeling to find the best fit gravity response.

1) In the first series of models, all of the subsurface load was assumed to be located in the asthenosphere. The asthenosphere was divided into two parts, the western part being less dense than the eastern part (Fig. 10 and Table 4) (Schmandt and Rumphreys, 2010; Mooney and Kaban, 2010). The boundary between the two mantle domains is modeled as a vertical interface, which in the best fit models is found to lie close to the Rocky Mountain Front Range border with the Denver basin (with an uncertainty of ±20 km in the east-west direction). The density contrast between the eastern and western asthenosphere mantle required to fit the long-wavelength shape of the Bouguer gravity anomaly is 0.02±0.002 g/cc for the central and south profiles, and 0.01±0.002 g/cc for the north profile. Varying the mantle density within the reasonable range of 3.2-3.4 g/cc makes little difference in the modeled anomaly, so long as the western mantle is 0.01-.02 g/cc less dense that the eastern mantle. The possibility of having more density domains within the asthenosphere was evaluated, but it was found that the additional complexity does not improve the fit to the long-wavelength gravity anomaly.
2) In the second series of models, all of the subsurface load was assumed to be located in the lithospheric mantle. Initial models attempted a simple division of the lithospheric mantle into eastern and western block, but further refinement into four blocks (WLM, LM1, LM2, and ELM) was ultimately required to fit the shape of the Bouguer gravity anomaly (Fig. 11 and Table 5). A relatively low density block (LM1) is located beneath the Front Range with a density of 3.1-3.16 g/cc, depending on the profile. The location of block LM1 shifts progressively to the west going from the north profile to the south. The density of the WLM block (west of LM1) decreases to the south from 3.23 to 3.21 g/cc. Blocks LM2 (3.23-3.24 g/cc, 100-450 km) and ELM (3.26 g/cc, east of LM2), below the Denver Basin and western Great Plains respectively, model a progressive

density decrease from east to west. Although this westward density decrease is modeled as a series of blocks, it is possible that it is instead a uniform gradient.

3) In the third series of models, all of the buoyant load was placed in the lower crust. The lower crust was divided into four blocks (WLC, LC1, LC2, and ELC), using the same block location and width, as in the second family of models (Fig. 12 and Table 6). The LC1 block below the Rocky Mountains has a density ranging from 2.76 to 2.89, and shifts progressively toward the west in the north-south direction. The density of block WLC (west of LC1) decreases to the south from 2.92 to 2.9 g/cc. The two eastern blocks LC2 (2.95-2.96 g/cc, 110-450 km) and ELC (3 g/cc, east of LC2) represent a density decrease moving from the western Great Plains to the Denver basin area.
4) In the fourth series of models, the entire load causing the Bouguer gravity minimum was placed in the upper crust, including the Front Range topographic part (Fig. 13 and Table 7). Initial models attempted a simple division of the upper crust into eastern and western block, but further refinement into four blocks (WUC, UC1, UC2, and EUC) was ultimately required to fit the shape of the Bouguer gravity anomaly. The UC1 block located within the Front Range Uplift has a density of 2.63-2.7 g/cc, and shifts progressively toward the west as in the previous two families of models. The density of the WUC (west of UC1) decreases to the south from 2.71 to 2.7 g/cc. Blocks UC2 (2.75 g/cc, 140-450 km) and EUC (2.8 g/cc, east of UC2) are located below the Denver Basin and western Great Plains respectively. The upper crust density has a general trend of decreasing from east (2.8 g/cc) to west (2.7 g/cc) for all the three gravity models.

10. Discussion

The deepest interface estimated from the spectral analysis for the three profiles (at 132-153 km depth) is interpreted to represent the base of the lithosphere. This is slightly less than

the 150-200 km lithosphere thickness beneath the Rocky Mountains estimated from P-wave tomography and the CD-ROM refraction profile data (Dueker et al., 2001; Karlstrom et al., 2005).

According to the available seismic refraction data (Keller et al., 1998), receiver functions (Sheehan et al., 1995), and EarthScope data (Gilbert, 2012), which were collected in the vicinity of the three profiles (no further than 42 km), the base of the crust in Colorado is estimated to be at depths of 37 to 53 km. The second deep interface estimated from the spectral analysis of 47.2±2.2 km on the central profile is the closest to the average previous seismic estimates. The second interface at 55.1 km depth on the south profile has a big uncertainty of ±6.5 km (based on the slope variation) and fits the seismic data as well. A high P-wave velocity layer is present in the lower crust at 35-55 km depth (Snelson et al., 2005; Rumpfhuber and Keller, 2009; Gilbert, 2012). The north profile value for the second deep interface of 35.1±1.1 km correlates with the top of this layer.

Some interfaces resolved in the power spectra, such as those at 8.7±1.7 and 3.2 km depth (north profile), 7.9±3.5 km (central), and 4.2±1.3 km (south), are in the upper crystalline crust, but no lithological contacts are identified that correlate with the depth at these interfaces.

The interfaces shallower than 3 km lie within or at the bottom of the sedimentary section, and are interpreted to represent boundaries between stratigraphic units. For example, the average depths to Precambrian basement for the central (2.1±0.7 km) and south (0.7±0.2 km) profiles are consistent with interpretations based on available well-log data (657-672 m depth, cogcc.state.co.us: Table A1) and basement structure map by Hemborg (1996).

Attempts to fit the long-wavelength Bouguer gravity low across the Denver Basin and Front Range Uplift entirely by flexural subsidence in the Denver Basin require too large elastic thicknesses of 128-162 km and 8-10 km deflection of the basin, even for the

continental lithosphere. Egan and Urquhart (1994) argued that modeling of segments through major Laramide structures implies that the elastic thickness of the lithosphere was very low (T_e = 5 km) during deformation. Macario et al. (1995) estimated T_e values for the western (30-39 km) and eastern Alps (33-40 km). McKenzie and Fairhead (1997) argue that the elastic thickness of continental lithosphere cannot exceed 25 km, except for the Himalayas (42 km). Stewart and Watts (1997) found different elastic thicknesses for several mountain ranges: the southern Appalachians (40-70 km), the Andes (5-85 km), the Alps (5-30 km), the Romanian Carpathians (5-20 km). The required loads of 4-5 x 10^{13} N/m are similar to the calculated loads (3.63-4.65 x 10^{13}) of the current topography west of the Denver Basin.

Assuming the crust-mantle boundary maintains the similar shape as the Precambrian basement in the Denver basin part of the profiles, the crystalline crust west of the Front Range uplift maintains a uniform thickness. However, due to flexure and filling of the Denver Basin, the total crust thickness increases from the eastern end of the profiles (about 44 km) to the western end reaching a thickness of >50 km beneath the Rockies (Snelson et al., 2005; Levander et al., 2005). However, this does not account entirely for the increase in magnitude of the long-wavelength gravity anomaly to the west. Modifying the shape of the crust-mantle and mid-crustal boundaries can provide a flexural fit to the gravity anomaly magnitude and slope, but this requires that the Denver Basin is deeper by as much as 5-6 km (Figure 8).

Elastic thicknesses estimated for the basement-fit models for the central and south profiles (58-60 km) are smaller than for the north profile (80 km). The lower elastic thickness in the southern part of the Denver Basin area might be related to the northern extension of the Rio Grande rift. The higher elastic thickness on the northern profile implies that the rift does not extend further north than approximately the 40.6°N latitude.

The load magnitude of 2-5 x 10^{12} N/m is much smaller than the weight of the mountains of 3.63-4.65 x 10^{13} in these models. The line load location is found to be within the Rockies (at

positions 42-182 km on the profiles), not near the edge of the basin. The smaller load of 2 x 10^{12} N/m for the south profile than the required loads for the north (4 x 10^{12} N/m) and central (5 x 10^{12} N/m) profiles and its position (182 km) are most likely because the profile transects the very southern edge of the basin, where the basin gets shallower and the basin axis is shifted east relative to the central profile.

Flexural models attempting to fit the depth to the basement in the Denver basin, rather than the Bouguer gravity field, result in gravity anomalies of only about 30-60 mGal, much less than what is observed (about 400 mGal) (Figure 9). These models confirm previous suggestions that the large Bouguer gravity low centered on the highest topography in the Colorado Rocky Mountains cannot be explained without a large subsurface mass deficit. Seismic refraction data (Keller et al., 1998), body-wave tomography (Gilbert, 2012), and receiver functions (Sheehan et al., 1995), all suggest that the crustal root beneath the Rocky Mountains is insufficient to account for the required mass deficit. The mass deficit has instead been variously interpreted as resulting from a shallow crustal source (Isaacson and Smithson, 1976; McCoy et al., 2005), a combination of lateral density variations in the crust and Moho relief (Li et al., 2002) and significant density variations in the mantle (Sheehan et al., 1995).

Forward gravity modeling indicates that the presence of low-density material beneath the Rocky Mountain Front Range is required to account for the significant Bouguer gravity minimum (-350-400 mGal) in this part of the profiles.

The models in which the mass deficiency is attributed entirely to the asthenospheric mantle (Table 4, Fig. 10) suggest that the western part of the asthenosphere (WAM) beneath the Front Range and extending further west should be less dense (0.01-0.02 g/cc), than the eastern part (EAM). This result agrees with the well-known difference between the tectonic western part of North America and the stable eastern part (Goes and van der Lee, 2002;

Schmandt and Rumphreys, 2010; Mooney and Kaban, 2010). However, these models are unable to simultaneously match the magnitude and the wavelength of the gravity anomaly on the western edge of the central and south profiles.

The models in which the mass deficiency is attributed entirely to the lithospheric mantle (Table 5, Fig. 11) require a density of 3.1-3.16 g/cc for lithospheric mantle block LM1 beneath the Front Range. This is reasonable, since peridotite has a density range of 3.1-3.4 g/cc (Lee, 2003; Sakamaki et al., 2011). There are two alternatives that the whole 50-km-thick block has such a low density: (1) it is possible that the entire lithospheric mantle has been modified by intrusions, (2) asthenospheric upwelling might partly decrease the density. However, Rumpfhuber and Keller (2009) estimate the uppermost mantle P-wave velocity to be at least 7.3 km/s, which maps to 3.06 g/cc for peridotite at upper mantle pressures and temperatures (Brocher, 2005). There are also shear wave low-velocity anomalies of -0.3 km/s in the uppermost mantle and lower crust in the western Colorado (Shen, W., M. H. Ritzwoller, and V. Schulte-Pelkum, A 3-D model of the crust and uppermost mantle beneath the Central and Western US by joint inversion of receiver functions and surface wave dispersion, submitted to *J. of Geof. Res.*, 2012). The lithosphere mantle blocks west (WLM) and east (LM2 and ELM) of the LM1 block have seismically and compositionally reasonable densities of 3.21-3.26 g/cc (higher than block LM1). However, these blocks have a lower lithosphere mantle density than considered for the other families of models (3.28 g/cc).

In models in which the subsurface mass deficit is constrained to lie entirely within the lower crust (Table 6, Fig. 12) the analogous lower crustal block LC1 beneath the Front Range has densities of 2.76-2.89 g/cc, which are lower than other blocks to the east (LC2 and ELC) and west of it (WLC). These densities are unlikely for the lower crust, because seismic studies of the Rocky Mountain region (Rumpfhuber and Keller, 2009) show a range of velocities for the lower crust of 6.6-7.3 km/s, which correspond to densities of 2.86-3.06 g/cc

(Brocher, 2005) with an average of 2.97 g/cc. In comparison, global average seismic velocities for continental orogens for the lower crust (approximately 20-50 km depth) are 6.4-7 km/s (Christensen and Mooney, 1995), corresponding to densities of 2.81-2.97 g/cc (Brocher, 2005). The densities for the LC1 block in the models overlap with all of the seismic results, but are at the low end of the range, and there is a relatively little overlap with the Rocky Mountain seismic data (Rumpfhuber and Keller, 2009). The other lower crust blocks (WLC, LC2, and ELC) have densities of 2.9-3.0 g/cc, and these values agree with the above mentioned seismic velocities.

Similarly, models in which the mass deficit is placed entirely in the upper crust require lower densities of 2.63-2.7 g/cc in the upper crust block UC1 beneath the Front Range Uplift and western Denver Basin compared to the other blocks west (WUC) and east of this region (UC2 and EUC) (Table 7, Fig. 13). Densities of less than 2.7 g/cc (lower limit for a granite rock) are possible for metamorphic rocks of the uppermost part of the upper crust, but not for the whole block UC1, which is about 20 km deep and includes almost all of the Rocky Mountain Front Range. Seismic studies (Christensen and Mooney, 1995; Rumpfhuber and Keller, 2009) estimate velocities for the upper crust range from 5.5 to 6.4 km/s (2.62-2.81 g/cc, Brocher, 2005) with an average of 2.76 g/cc in the Colorado Rocky Mountains. The upper crustal blocks west (WUC) and east (UC2 and EUC) of the UC1 block have seismically and compositionally reasonable densities of 2.7-2.8 g/cc.

Alternative models (not presented here) indicate that variations in the density values within each block of 0.01-0.03 g/cc are permissible, but the changes of >0.03 g/cc lead to unrealistically high/low densities according to the available density log and seismic data. Changing the shape of the density interfaces and the density block boundary position affects the gravity response depending on the depth: relatively shallow (up to 3 km depth) interfaces

might vary no more than 100 m and still match the gravity data reasonably well, deeper interfaces may be varied by no more than 1 km.

The four families of gravity models taken together (Figs. 10-13, Tables 4-7) demonstrate that the subsurface load is unlikely to be constrained to lie entirely within any one of the depth levels investigated. If the subsurface load lies entirely in the lithospheric mantle or crust, extremely low densities are required. The asthenosphere family of models is unable to simultaneously fit the magnitude and the wavelength of the gravity anomaly. The isostatic compensation of the high Southern Rocky Mountains results from a complex interplay in some combination between the low-density crust (upper or lower) and/or low-density upper mantle (lithosphere or asthenosphere).

11. Conclusions

Analysis of Bouguer gravity, well and seismic refraction data are used to construct subsurface tectonic models along three lithosphere-scale profiles trending across the Denver Basin from the western part of the Southern Rocky Mountains to the western Great Plains. The Bouguer gravity power spectra along each profile reveal five to six linear segments corresponding to subsurface density interfaces. The interfaces are interpreted to represent the base of the lithosphere, at average depths of 132 to 153 km, base of the crust (45-55 km), mid-crustal boundary (about 20 km), average Precambrian basement depth (1-2 km), and boundary between Pierre Shale and underlying Mesozoic and older sedimentary layers (-1-0 km).

Attempts to fit the long-wavelength Bouguer gravity low across the Denver Basin and Front Range Uplift entirely by flexural subsidence in the Denver Basin require too large elastic thicknesses of 128-162 km and 8-10 km deflection of the basin. The required loads of 4-5 x 10^{13} N/m are similar to the calculated loads (3.63-4.65 x 10^{13}) of the current topography

west of the Denver Basin. The flexural shape of the Denver Basin can be fit with an elastic plate model having an elastic thickness ranging from 58-80 km and a line load ranging from magnitude 2-5 x 10^{12} N/m on each of the three profiles. The location of the line load is 90-115 km west of the Bouguer gravity minimum on each profile. The gravity response of the flexural models (-30-60 mGal) is not enough to agree with the observed negative Bouguer gravity anomaly of about -400 mGal.

The magnitude of the load in these flexural models is less than the present topography weight of 3.63-4.65 x 10^{13} N/m, indicating that the weight of the Rocky Mountain Front Range is only partially compensated by flexural isostasy. Since seismic data indicate a lack of a pronounced crustal root, a buoyant subsurface load is required.

Forward gravity models, supplemented with available well and seismic refraction data, are developed to test four end-member hypotheses as to the location of the buoyant subsurface load. The load is tested to lie entirely within the: (1) asthenosphere, (2) shallow lithosphere mantle, (3) lower crust, or (4) upper crust. The forward gravity models prove that the subsurface buoyant load is most likely partitioned in some combination between low-density crust and/or low-density upper mantle.

The models indicate abrupt crust thickening at the boundary between Rocky Mountains and Great Plains, from about 48 km beneath the Denver Basin to about 53 km beneath the Front Range Uplift, agreeing with the regional seismic data and implications of the previous studies.

TABLES

Table 1. Density interfaces in the Bouguer gravity power spectra

North Profile			
Minimum depth (km)	Maximum depth (km)	Average depth* (km)	Inferred interface
143.2	165.5	152.9±11.2	Base of lithosphere
35.5	37.7	35.1±1.1	Upper - Lower Crust
8.5	11.9	8.7±1.7	
4.7	4.7	3.2	
1.5	1.8	0.2±0.2	Pierre - Niobrara

Central Profile			
Minimum depth (km)	Maximum depth (km)	Average depth* (km)	Inferred interface
133.7	132.4	131.5 ± 0.7	Base of lithosphere
46.6	50.9	47.2 ± 2.2	Lower Crust - Mantle
6.1	13.0	7.9 ± 3.5	
3.0	4.4	2.1 ± 0.7	Sediments - Basement
1.6	2.4	0.4 ± 0.4	
0.7	1.1	(-0.7) ± 0.2	Pierre - Niobrara

South Profile			
Minimum depth (km)	Maximum depth (km)	Average depth* (km)	Inferred interface
125.3	165.5	143.8±20.1	Base of lithosphere
63.2	50.3	55.1±6.5	Lower Crust - Mantle
23.6	20.2	20.3±1.7	Upper - Lower Crust
7.0	4.5	4.2±1.3	
2.4	2.1	0.7±0.2	Sediments - Basement
0.8	1.0	(-0.7)±0.1	

* Depth below average elevation of profile

Table 2. Relationship of seismic velocities (Rumpfhuber and Keller, 2009) and densities according to Brocher (2005)

	Velocity (km/s)	Density (g/cc)
Upper crust	5.8 - 6.3	2.68 - 2.78
Lower crust	6.6 - 7.3	2.86 - 3.06
Uppermost mantle	7.3 -	3.06 -

Table 3. Results of flexural modeling

Gravity-fit models				
Profile	Rigidity (10^{25} Nm)	Elastic Thickness (km)	Load Magnitude (10^{13} N/m)	Position of the load (km)
North	2.09	133	4	51
Central	1.86	128	4.2	86
South	3.78	162	5	27

Basement-fit models				
Profile	Rigidity (10^{24} Nm)	Elastic Thickness (km)	Load Magnitude (10^{12} N/m)	Position of the load (km)
North	4.55	80	4	86
Central	1.92	60	5	42
South	1.73	58	2	182

Table 4. Gravity model block geometry: Asthenospheric mantle models

Profile	Block WAM density (g/cc)	Block boundary position (km)	Block EAM density (g/cc)
North	3.3	175	3.31
Central	3.3	175	3.32
South	3.3	165	3.32

Table 5. Gravity model block geometry: Lithospheric mantle models

Profile	Block WLM density (g/cc)	Block boundary position (km)	Block LM1 density (g/cc)	Block boundary position (km)	Block LM2 density (g/cc)	Block boundary position (km)	Block ELM density (g/cc)
North	3.23	10	3.16	110	3.24	450	3.26
Central	3.22	-10	3.1	110	3.23	450	3.26
South	3.21	-50	3.14	100	3.23	450	3.26

Table 6. Gravity model block geometry: Lower crust models

Profile	Block WLC density (g/cc)	Block boundary position (km)	Block LC1 density (g/cc)	Block boundary position (km)	Block LC2 density (g/cc)	Block boundary position (km)	Block ELC density (g/cc)
North	2.92	10	2.89	120	2.96	440	3
Central	2.91	0	2.76	120	2.95	450	3
South	2.9	-10	2.84	110	2.95	440	3

Table 7. Gravity model block geometry: Upper crust models

Profile	Block WUC density (g/cc)	Block boundary position (km)	Block UC1 density (g/cc)	Block boundary position (km)	Block UC2 density (g/cc)	Block boundary position (km)	Block EUC density (g/cc)
North	2.71	10	2.7	150	2.75	440	2.8
Central	2.7	0	2.63	140	2.75	450	2.8
South	2.7	-10	2.67	140	2.75	450	2.8

FIGURES

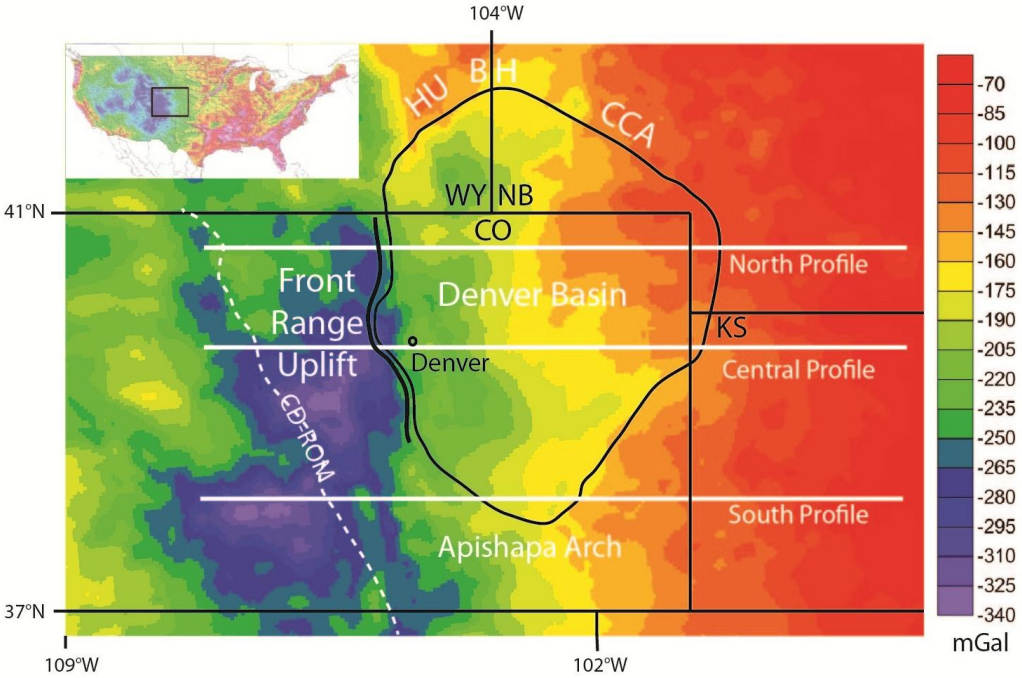

Figure 1. Bouguer gravity map showing outline of the Denver Basin (black line), Rocky Mountain Front Range, three gravity profiles (white lines), and the CD-ROM refraction profile (white dashed line) from Rumpfhuber and Keller (2009). HU = Hartville Uplift, BH = Black Hills, CCA = Chadron-Cambridge Arch, WY = Wyoming, NB = Nebraska, CO = Colorado, KS = Kansas.

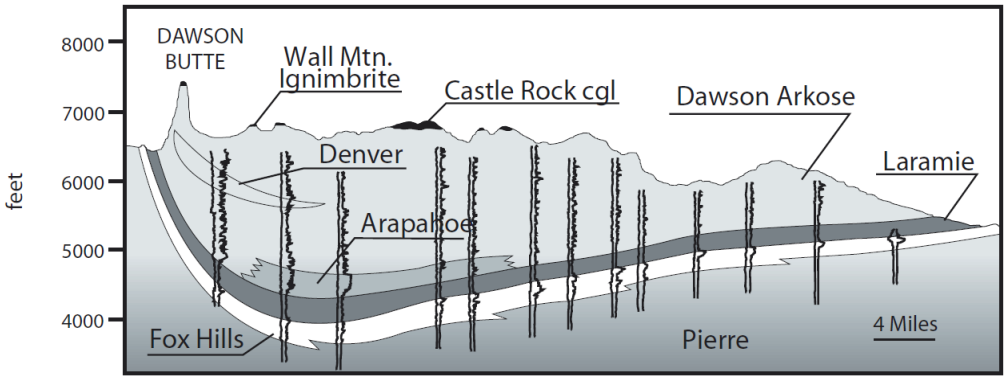

Figure 2. Cross section of the Denver Basin illustrating its stratigraphic nomenclature (Raynolds, 2002).

ERA	PERIOD	FORMATION
Cenozoic	Eocene	Castle Rock Conglomerate
		Wall Moutain Ignimbrite
		Dawson Arkose (D2)
	Paleocene	Denver (D1)
		Arapahoe (D1)
Mesozoic	Cretaceous	Laramie
		Fox Hills
		Pierre Shale
		Niobrara
		Benton Group
		Dakota Group

Figure 3. Generalized stratigraphic column of the upper section of the Denver Basin fill (after Raynolds et al., 2007).

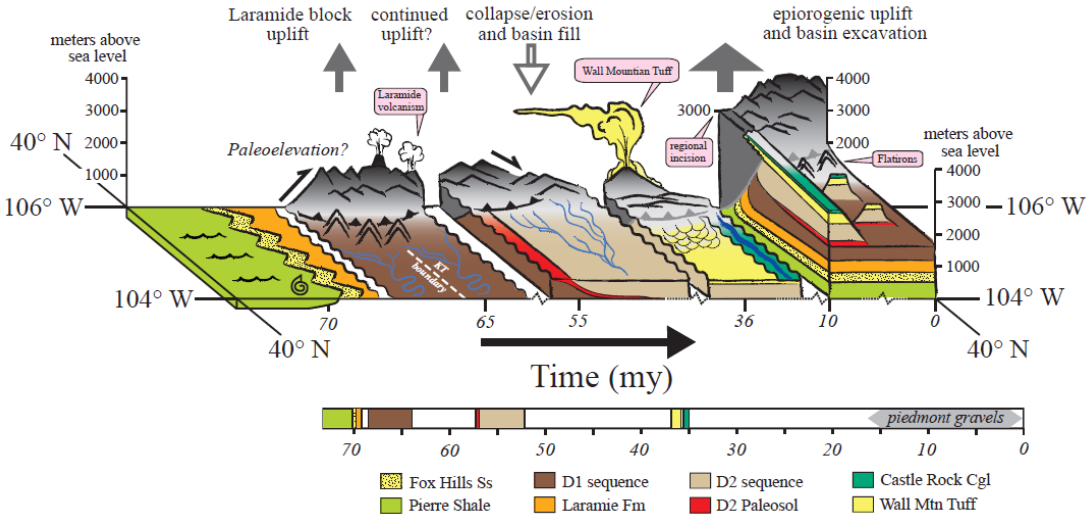

Figure 4. Space-time-elevation diagram showing the evolution of topography in the Colorado Front Range and the Denver Basin. The diagram is fixed in space at latitude 40°N and between longitudes 104°W and 107°W. It scrolls through time from 75 Ma on the left to the present on the right, and Denver moves with time on the x-axis. The diagram shows the Interior Seaway and sea level conditions extending to ca. 68 Ma, followed by abrupt and episodic uplifts to the west. Between ca. 40 and 50 Ma, the area witnessed orogenic collapse and regional beveling. This was followed by late-stage regional uplift and basin exhumation (Raynolds et al, 2007).

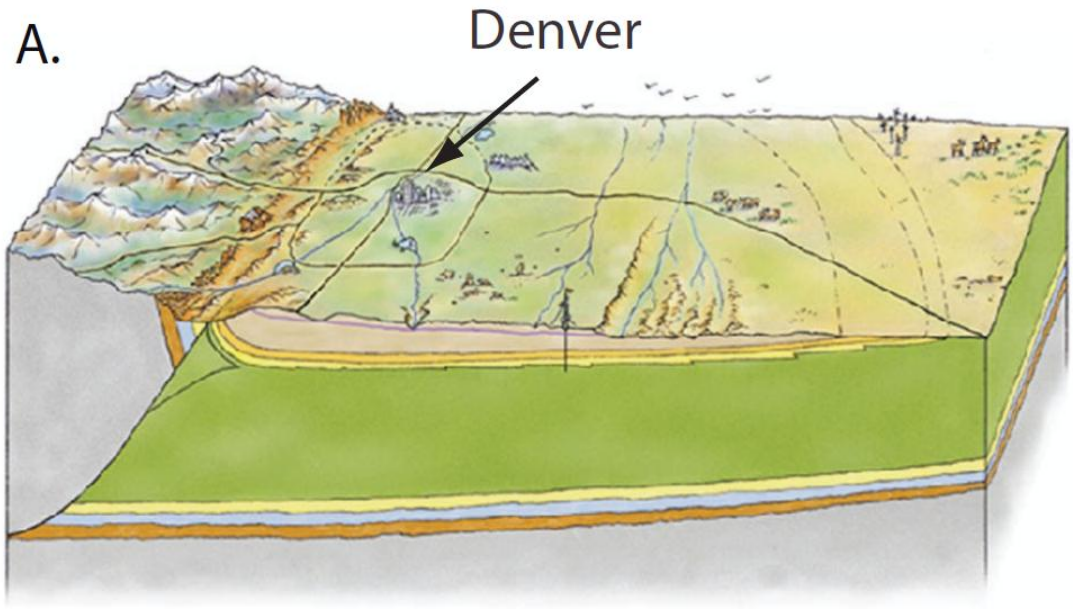

Figure 5. Three-dimensional view of strata in the Denver Basin. Image is schematic; the thick green unit denotes deposits of the Cretaceous Interior Seaway (Raynolds et al, 2007).

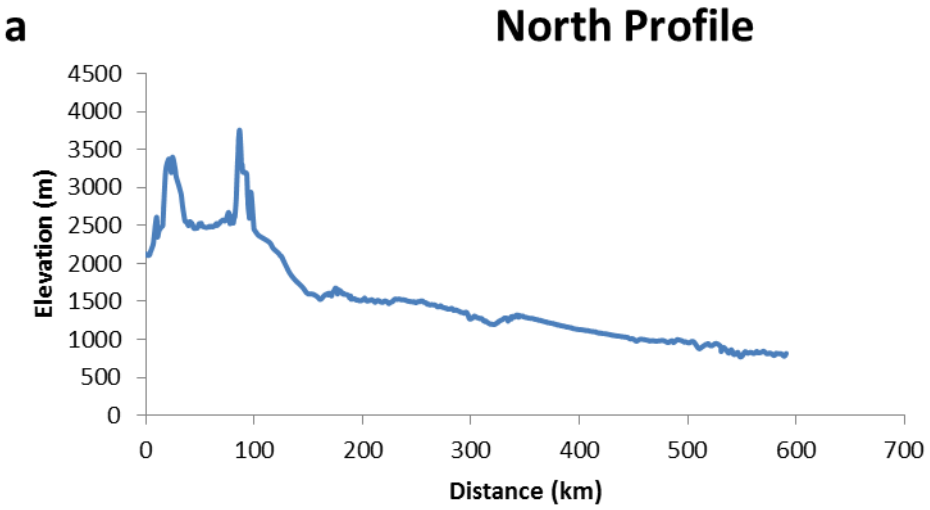

b

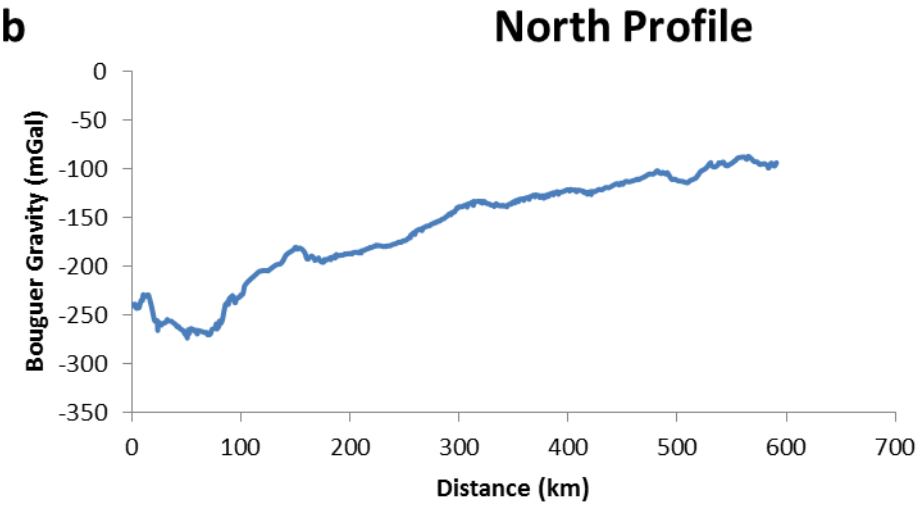
North Profile
Bouguer Gravity (mGal)
0
-50
-100
-150
-200
-250
-300
-350
0
100
200
300
400
500
600
700
Distance (km)

c

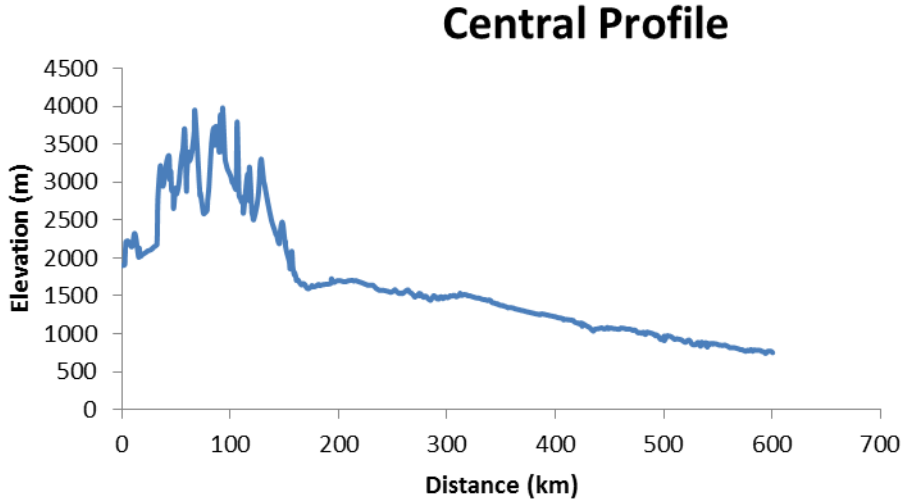
Central Profile
Elevation (m)
4500
4000
3500
3000
2500
2000
1500
1000
500
0
0
100
200
300
400
500
600
700
Distance (km)

d

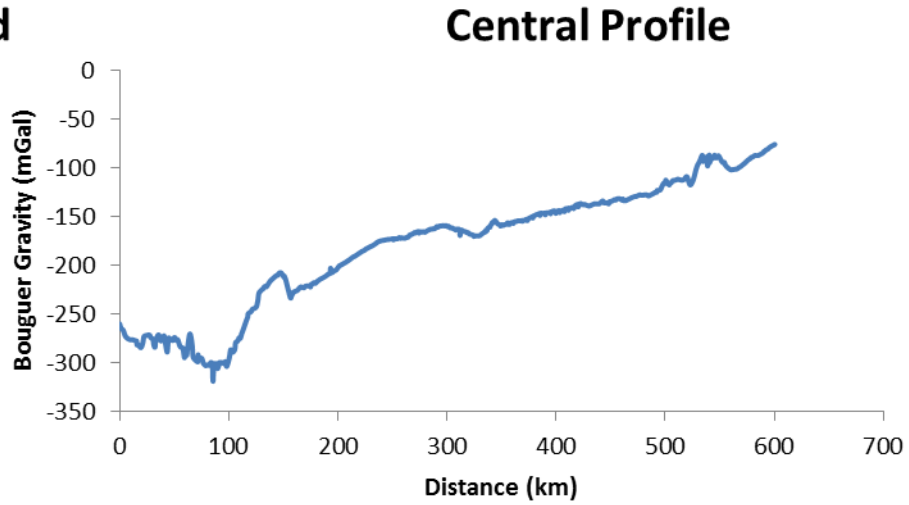
Central Profile
Bouguer Gravity (mGal)
0
-50
-100
-150
-200
-250
-300
-350
0
100
200
300
400
500
600
700
Distance (km)

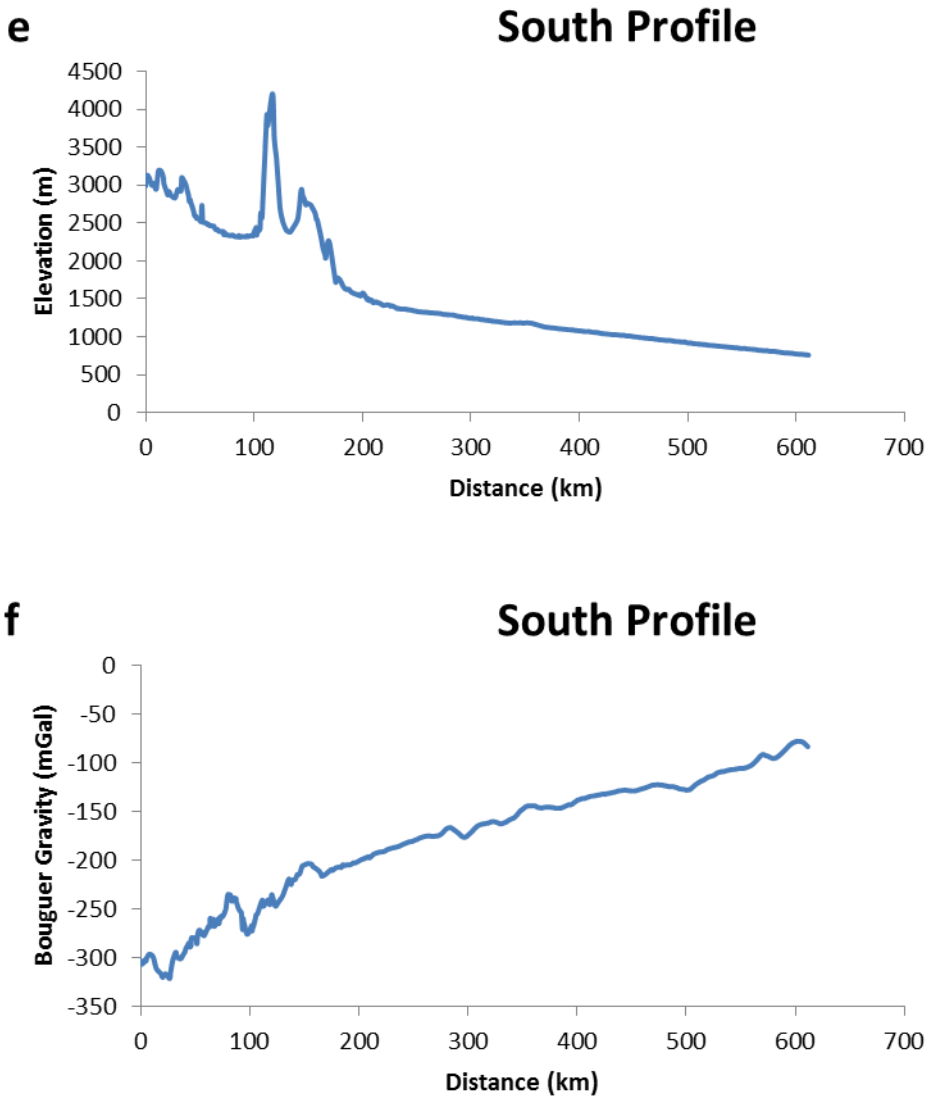

Figure 6. Topography (a, c, e) and Bouguer gravity (b, d, f) profiles.

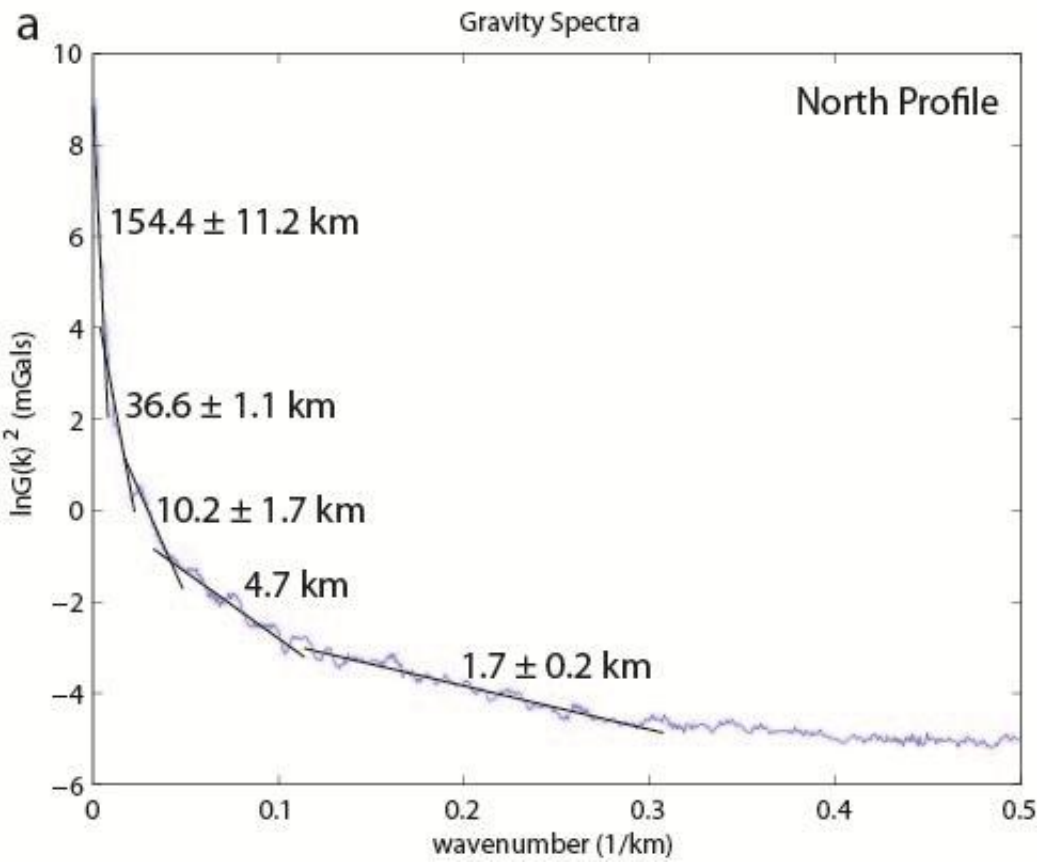
a
Gravity Spectra
North Profile
154.4 ± 11.2 km
36.6 ± 1.1 km
10.2 ± 1.7 km
4.7 km
1.7 ± 0.2 km
lnG(k) 2 (mGals)
wavenumber (1/km)

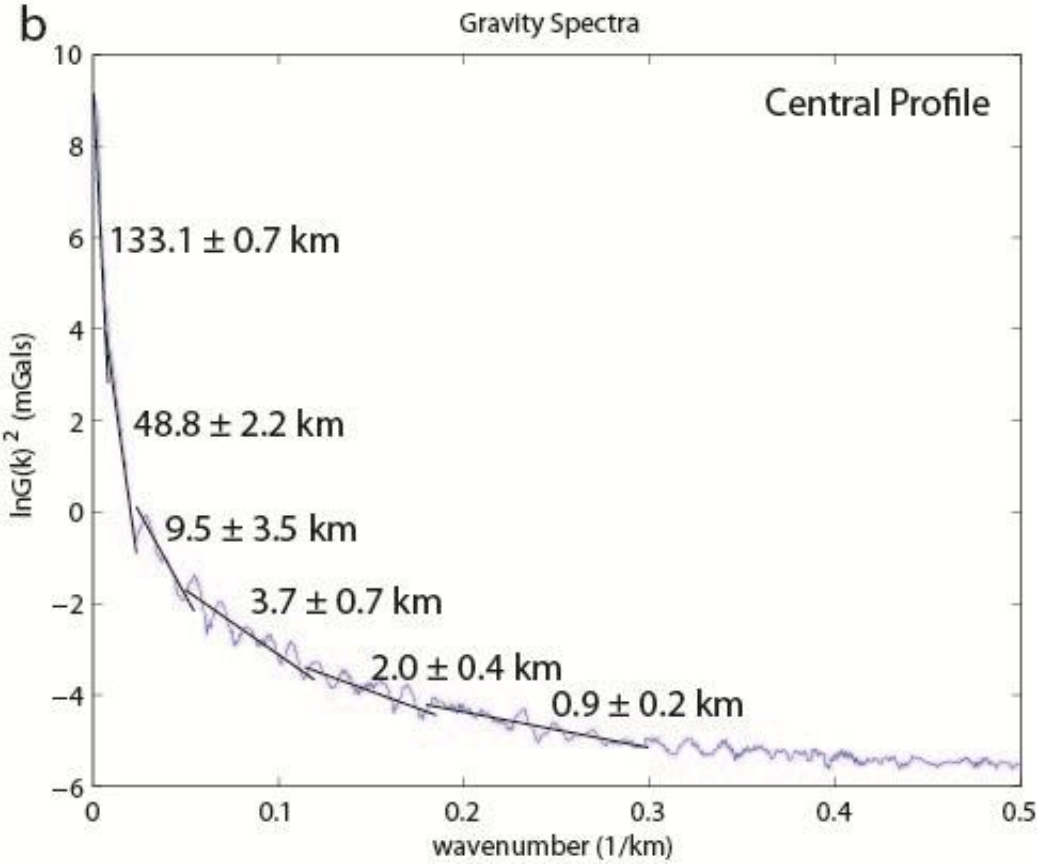
b
Gravity Spectra
Central Profile
133.1 ± 0.7 km
48.8 ± 2.2 km
9.5 ± 3.5 km
3.7 ± 0.7 km
2.0 ± 0.4 km
0.9 ± 0.2 km
lnG(k) 2 (mGals)
wavenumber (1/km)

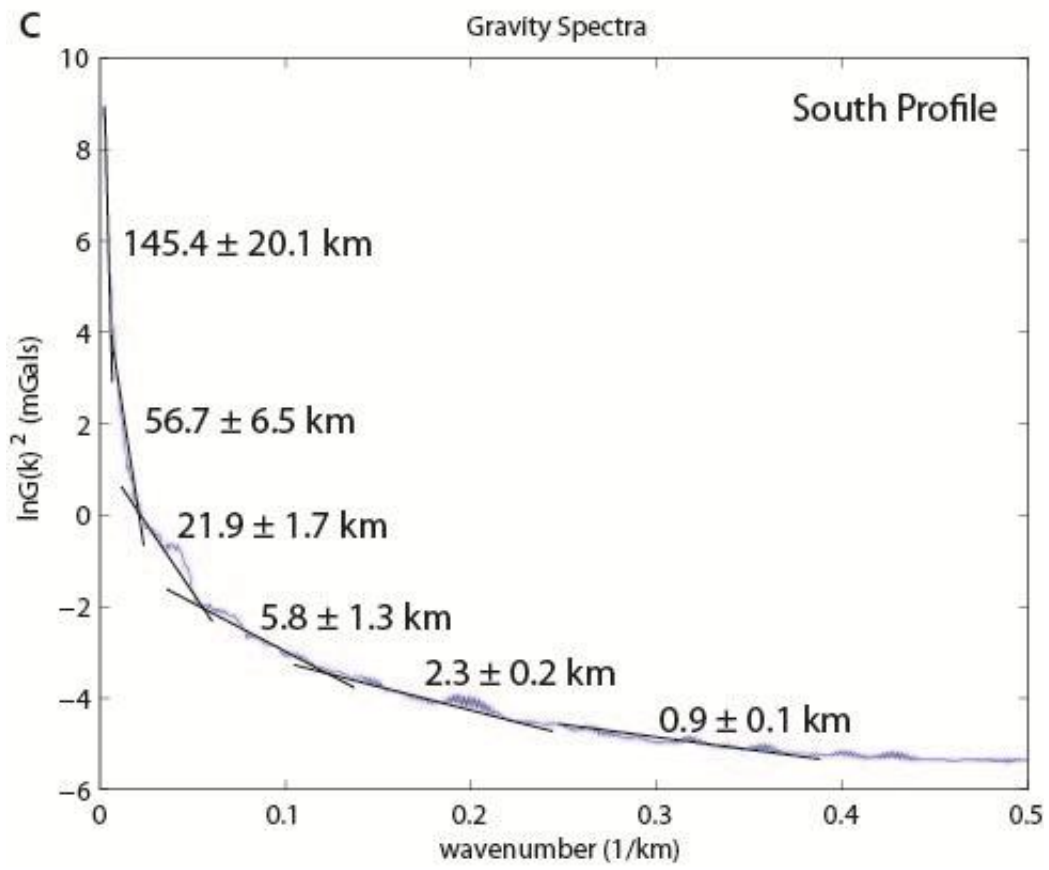

Figure 7. Bouguer gravity power spectra for the north (a), central (b), and south (c) profiles. Solid lines indicate linear segments of the spectra used to identify the depth to major density interfaces.

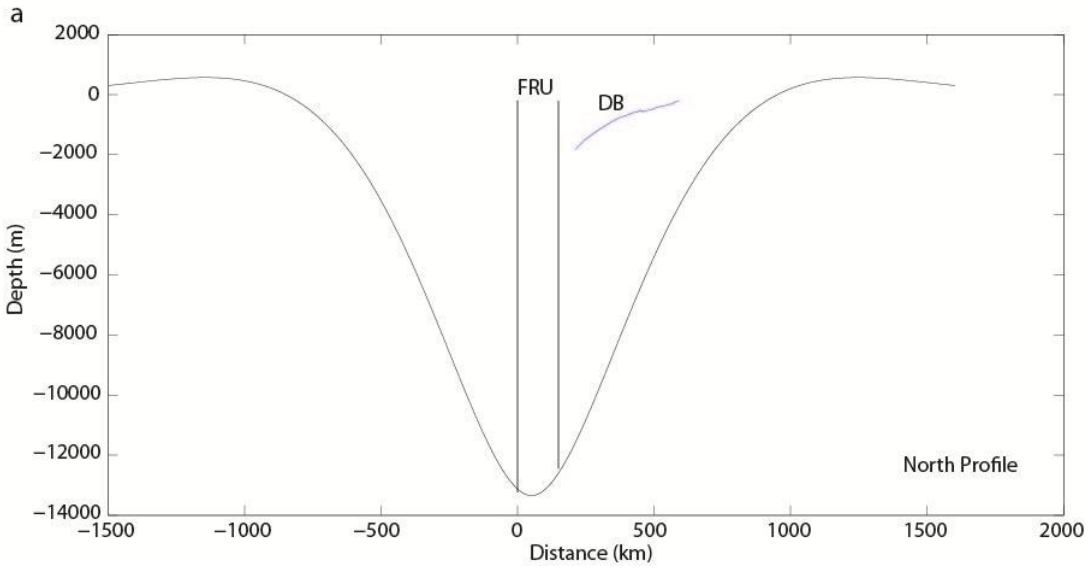

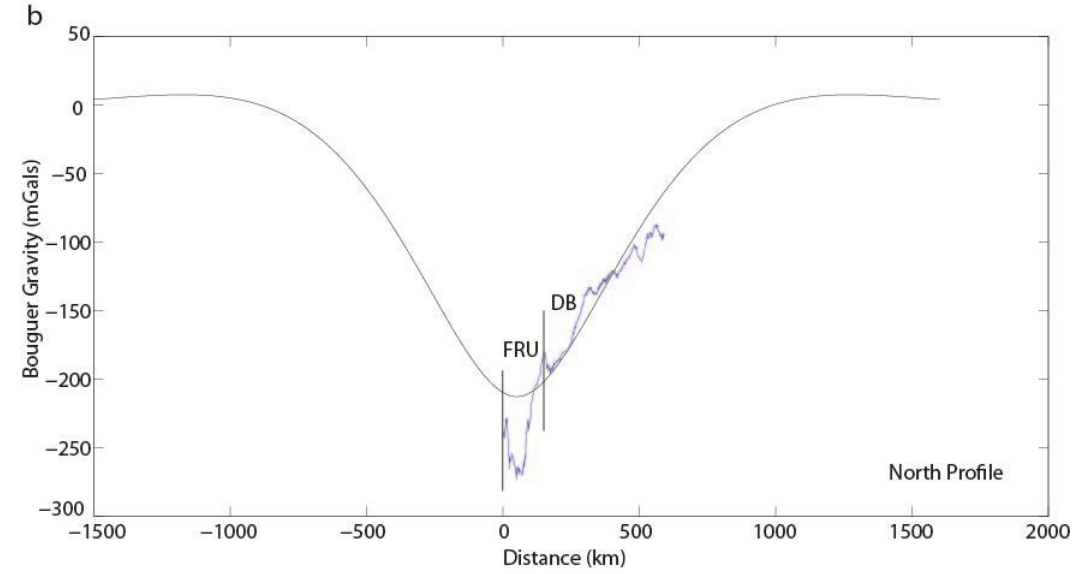
b
Bouguer Gravity (mGals)
50
0
−50
−100
−150
−200
−250
−300
FRU
DB
North Profile
−1500
−1000
−500
0
500
1000
1500
2000
Distance (km)

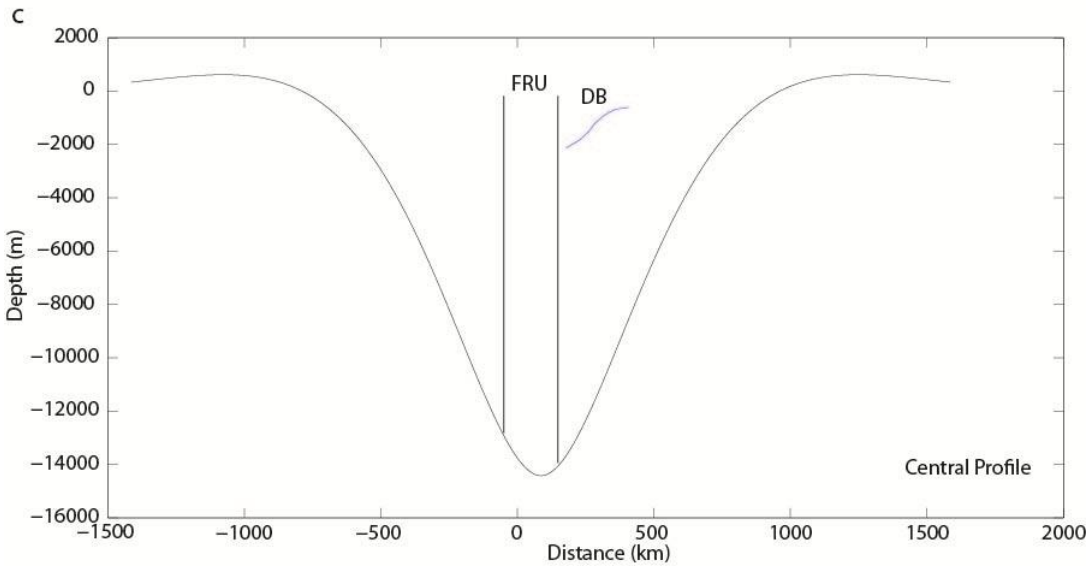
c
Depth (m)
2000
0
−2000
−4000
−6000
−8000
−10000
−12000
−14000
−16000
FRU
DB
Central Profile
−1500
−1000
−500
0
500
1000
1500
2000
Distance (km)

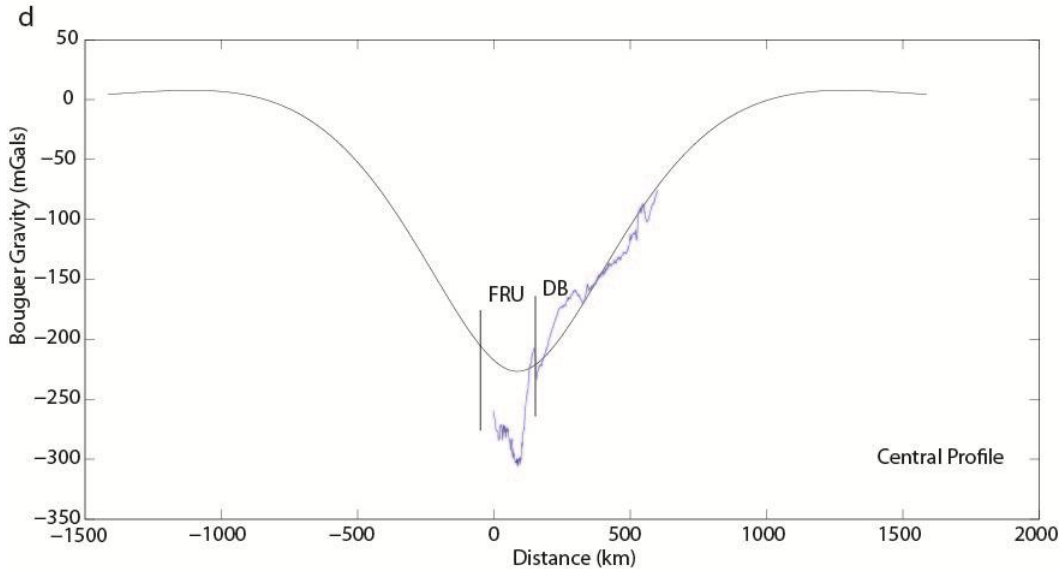
d
Bouguer Gravity (mGals)
50
0
−50
−100
−150
−200
−250
−300
−350
FRU
DB
Central Profile
−1500
−1000
−500
0
500
1000
1500
2000
Distance (km)

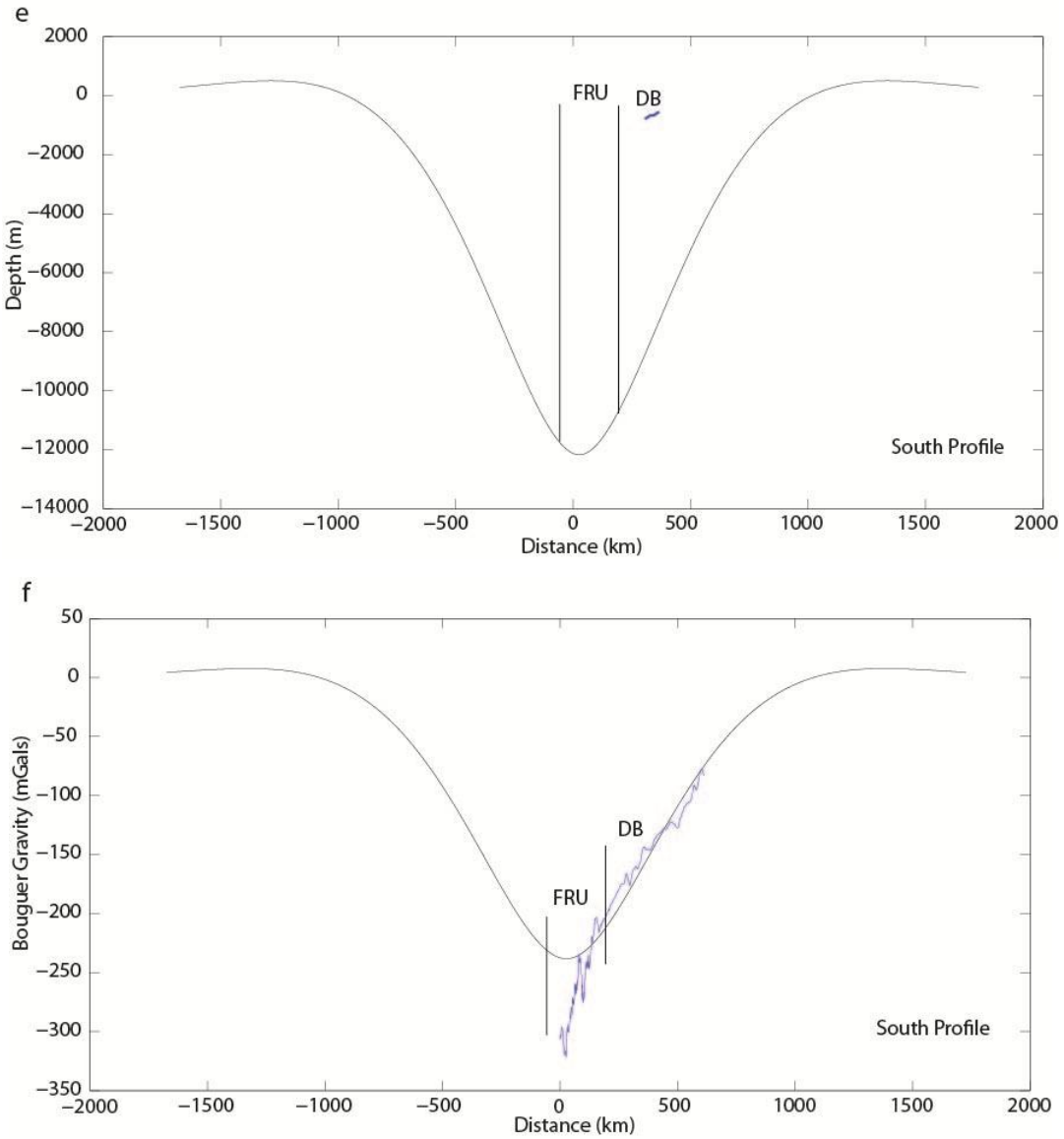

Figure 8. Flexural models fitting the Bouguer gravity profiles (a, c, e) and their gravity response (b, d, f). Blue lines are observed flexural shape of Precambrian basement and Bouguer gravity field. Black lines are calculated flexural profiles and their gravity response. FRU = Front Range Uplift, DB = Denver Basin.

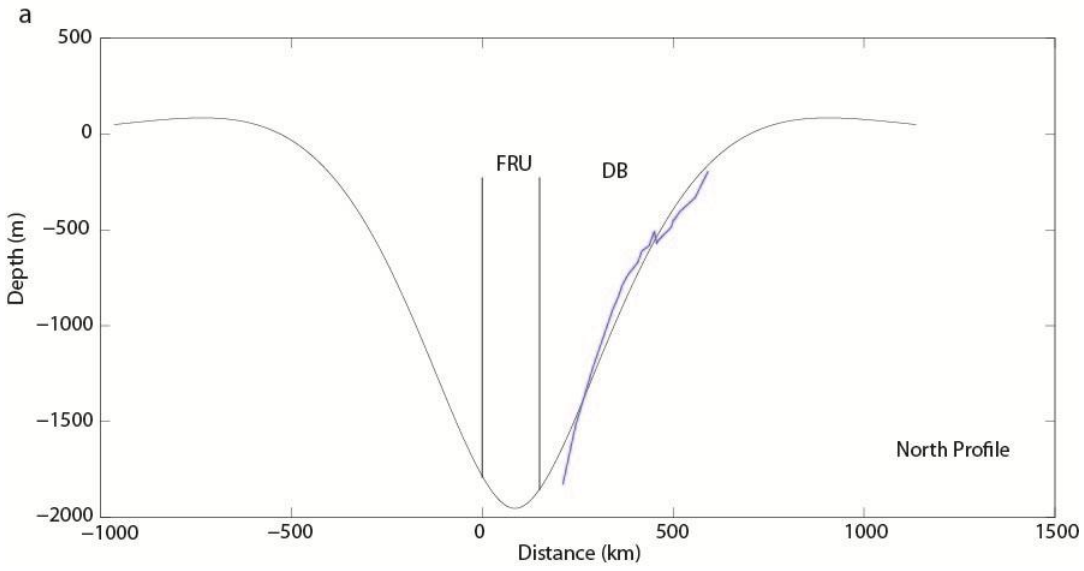
a
500
0
−500
−1000
−1500
−2000
Depth (m)
FRU
DB
North Profile
−1000
−500
0
500
1000
1500
Distance (km)

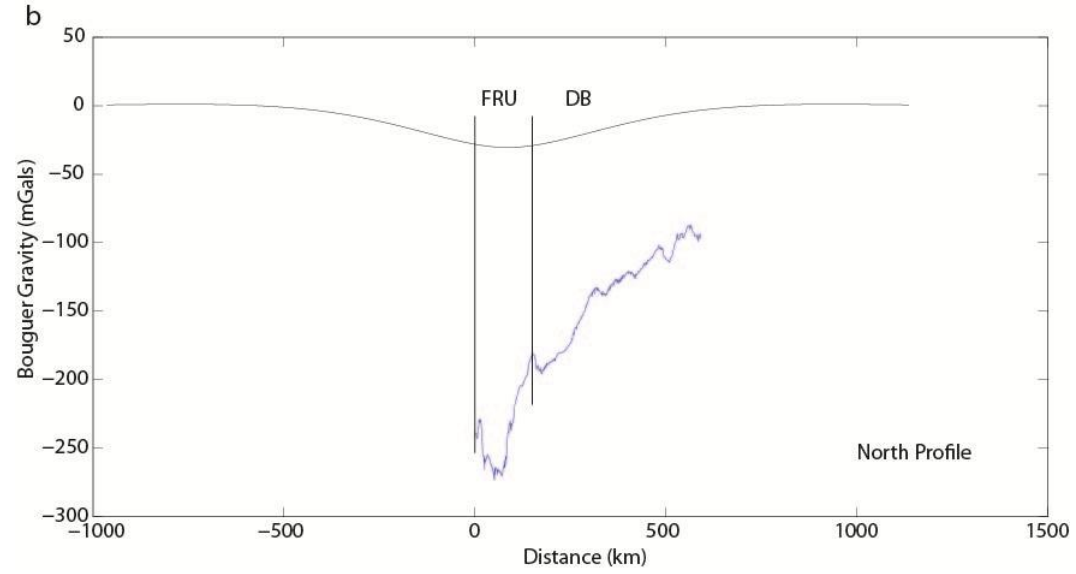
b
50
0
−50
−100
−150
−200
−250
−300
Bouguer Gravity (mGals)
FRU
DB
North Profile
−1000
−500
0
500
1000
1500
Distance (km)

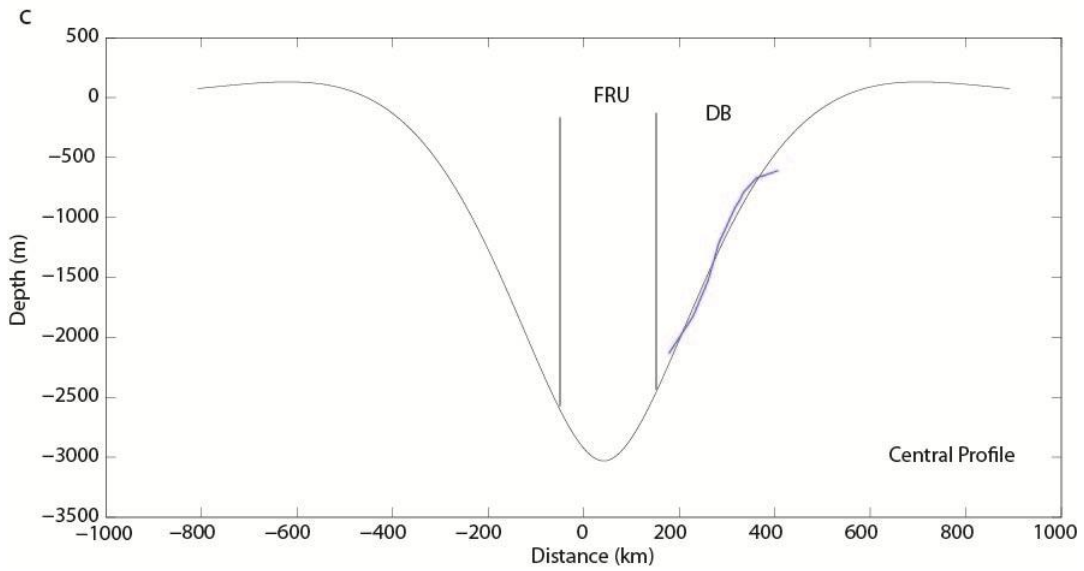
c
500
0
−500
−1000
−1500
−2000
−2500
−3000
−3500
Depth (m)
FRU
DB
Central Profile
−1000
−800
−600
−400
−200
0
200
400
600
800
1000
Distance (km)

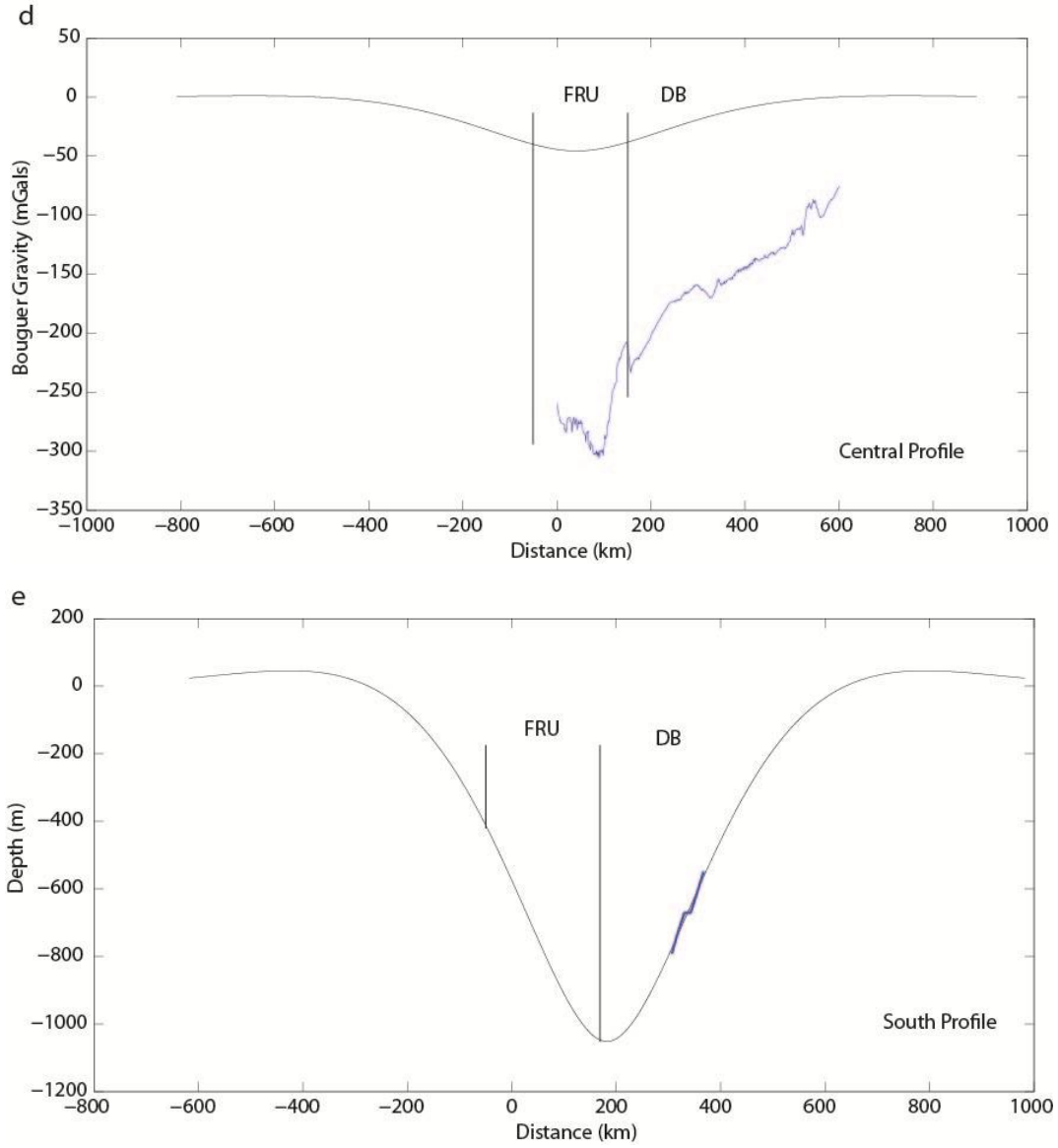
d
50
0
−50
−100
−150
−200
−250
−300
−350
Bouguer Gravity (mGals)
FRU
DB
Central Profile
−1000
−800
−600
−400
−200
0
200
400
600
800
1000
Distance (km)
e
200
0
−200
−400
−600
−800
−1000
−1200
Depth (m)
FRU
DB
South Profile
−800
−600
−400
−200
0
200
400
600
800
1000
Distance (km)

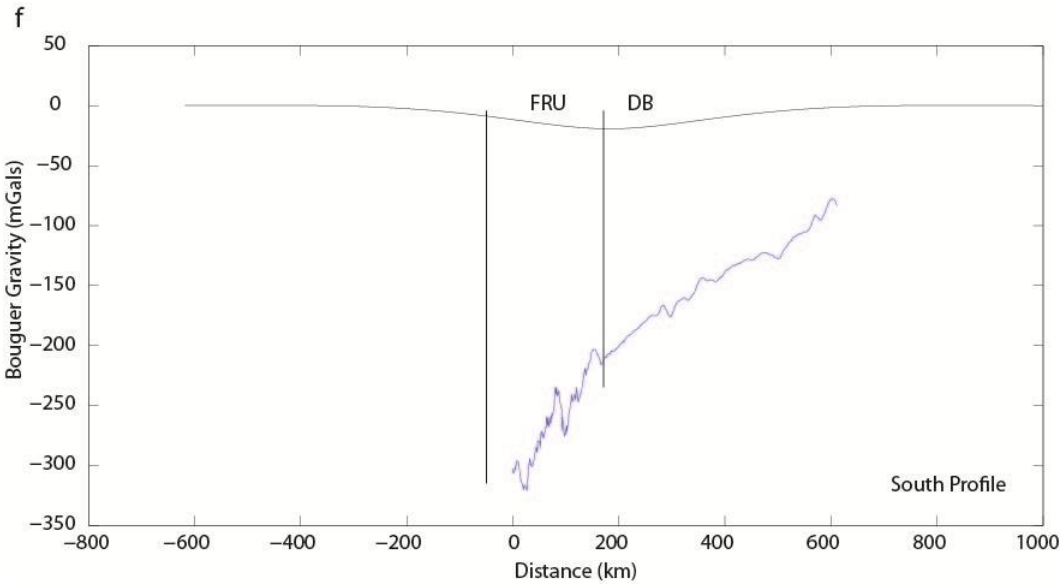

Figure 9. Flexural models fitting the top of Precambrian basement (a, c, e) and their gravity response (b, d, f). Blue lines are observed flexural shape of Precambrian basement and Bouguer gravity field. Black lines are calculated flexural profiles and their gravity response. FRU = Front Range Uplift, DB = Denver Basin.

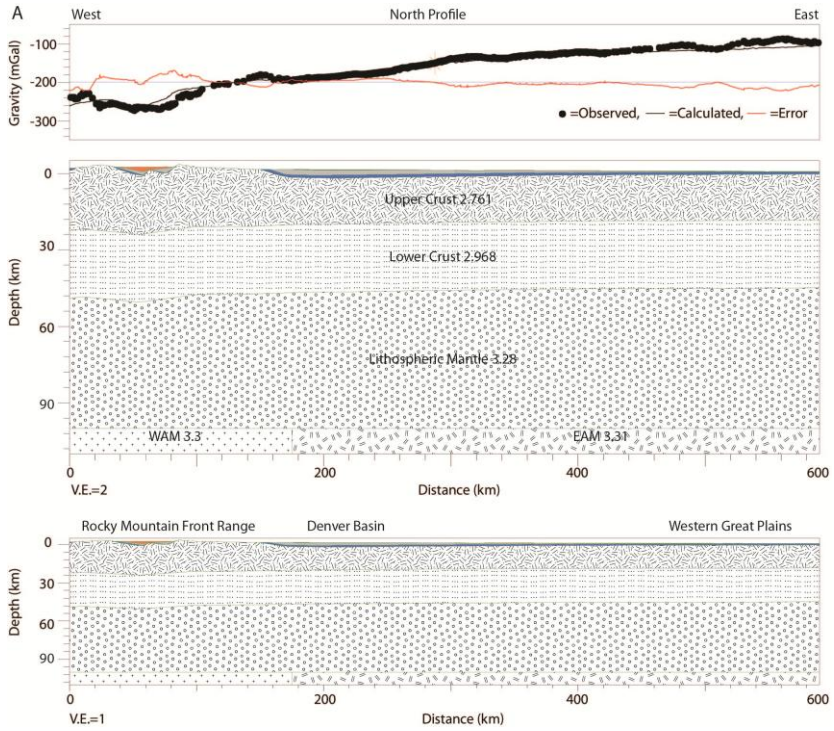

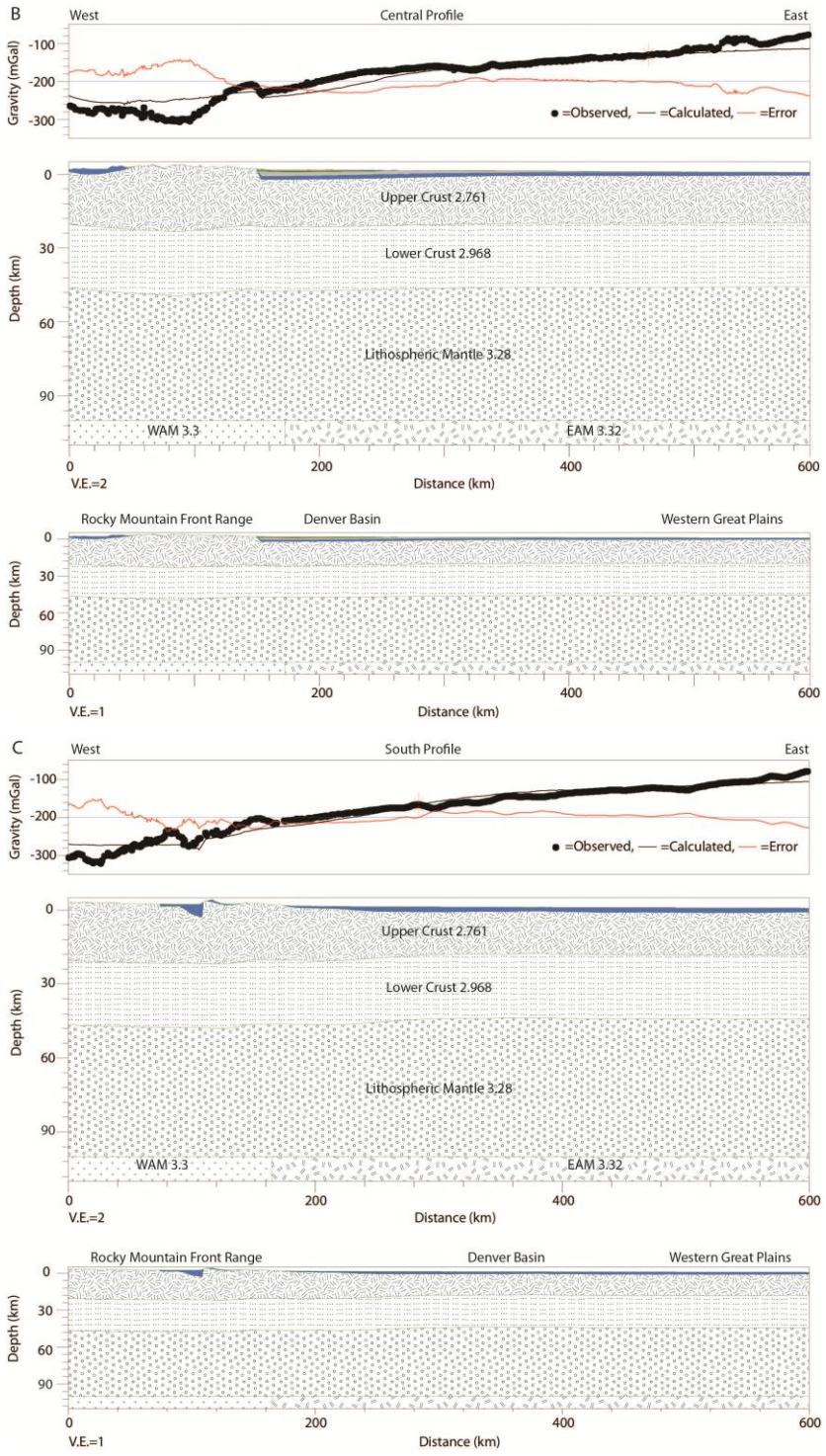

Figure 10. Forward gravity models – mass deficiency within the asthenosphere.

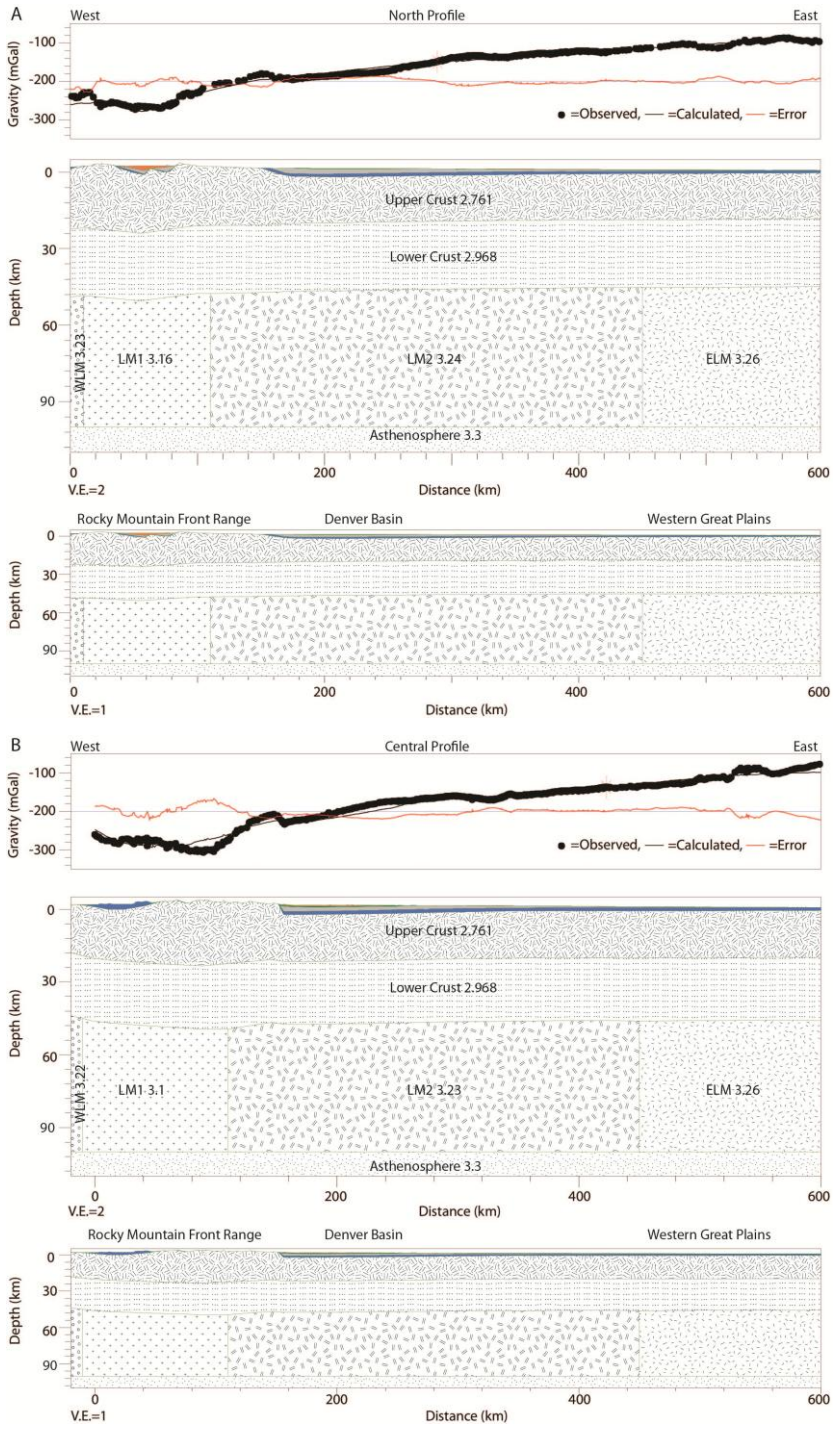
A
West
North Profile
East
Gravity (mGal)
-100
-200
-300
● =Observed, — =Calculated, — =Error
Depth (km)
0
30
60
90
Upper Crust 2.761
Lower Crust 2.968
WLM 3.23
LM1 3.16
LM2 3.24
ELM 3.26
Asthenosphere 3.3
0
200
400
600
V.E.=2
Distance (km)
Rocky Mountain Front Range
Denver Basin
Western Great Plains
V.E.=1
B
West
Central Profile
East
WLM 3.22
LM1 3.1
LM2 3.23

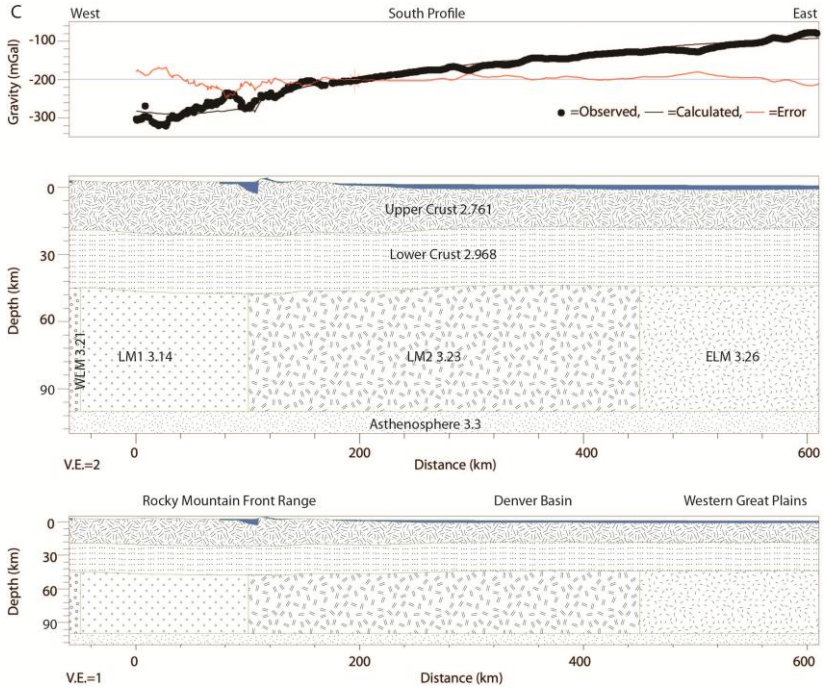

Figure 11. Forward gravity models – mass deficiency within the lithospheric mantle.

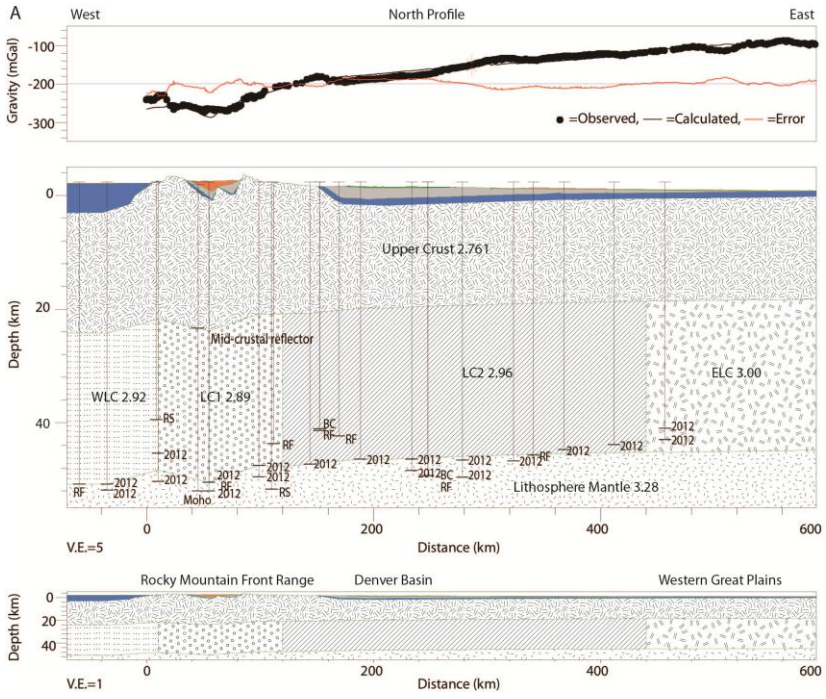

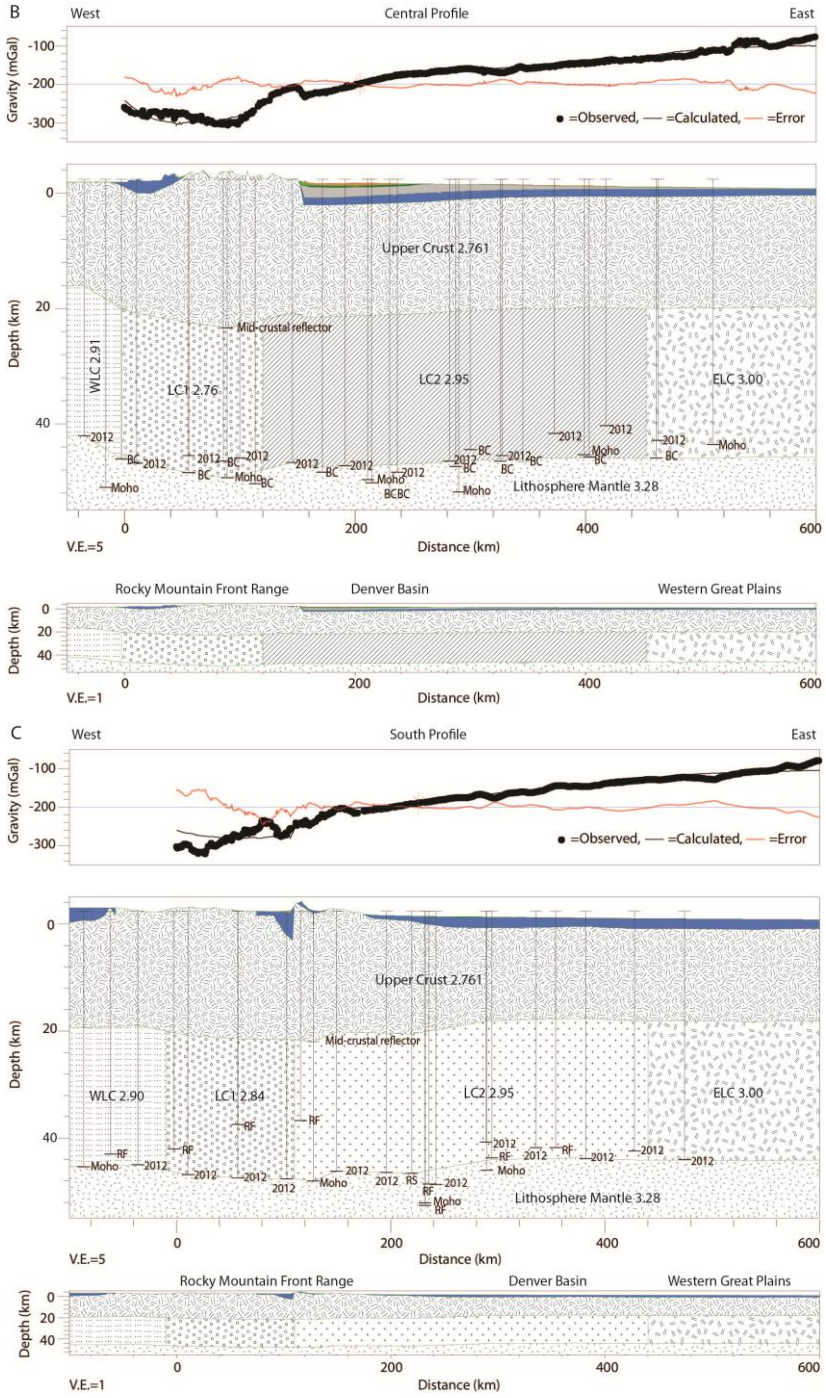

Figure 12. Forward gravity models – mass deficiency within the lower crust.

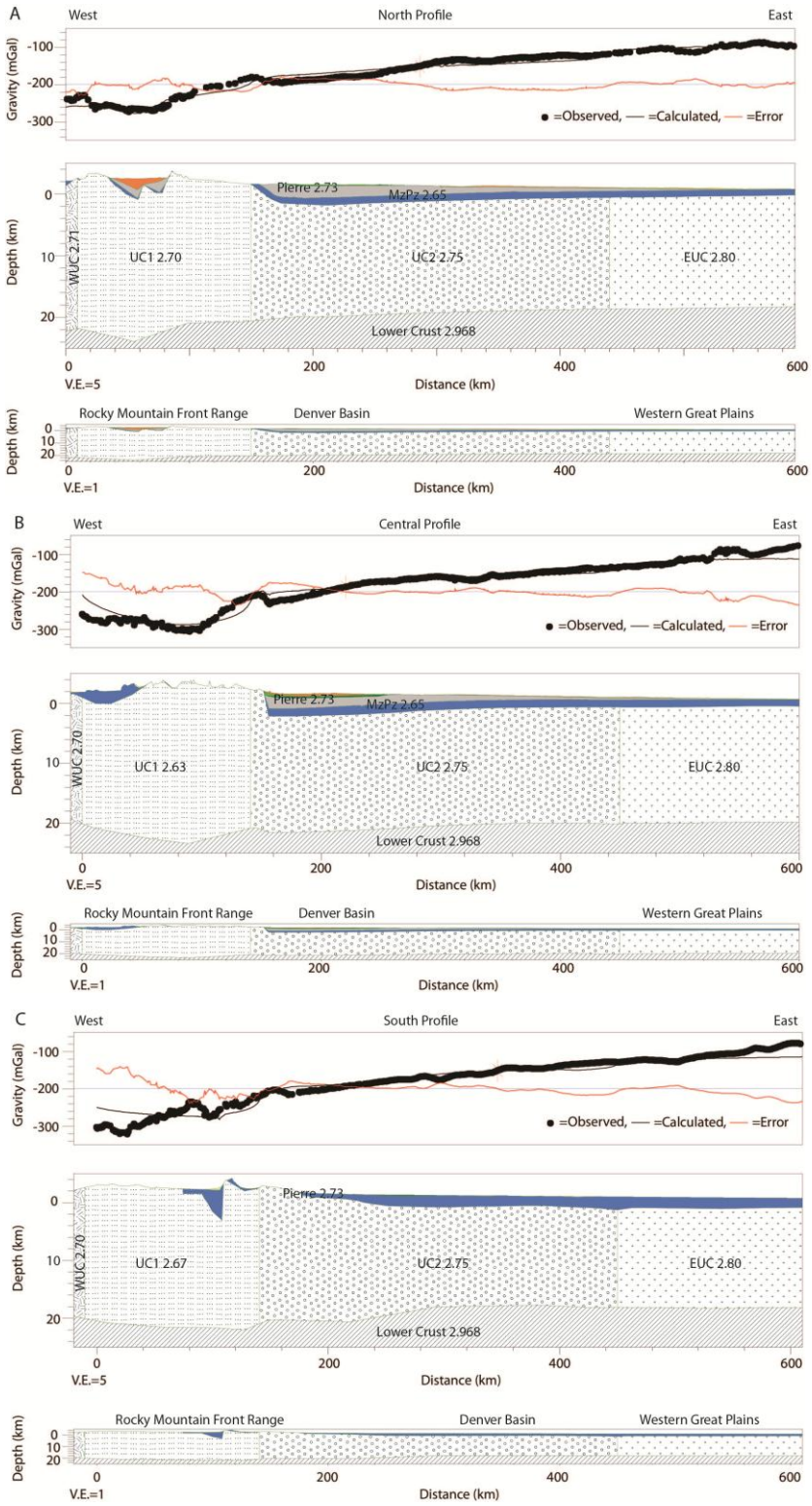

Figure 13. Forward gravity models – mass deficiency within the upper crust.

REFERENCES

Allenby, R. J., and C. C. Schnetzler (1983), United States crustal thickness, *Tectonophysics*, *93*(1-2), 13-31.

Angevine, C. L., and K. M. Flanagan (1987), Buoyant sub-surface loading in the Great Plains foreland basin, *Nature*, *327*, 137-139.

Babits, S. J. (1987), Gravity anomalies and lithospheric flexure beneath the Denver Basin: Evidence for a buoyant subcrustal load, M.S. thesis, Dep. of Geol. and Geophys., Univ. of Wyoming, Laramie, Wyoming, USA.

Banks, R. J., R. L. Parker, and S. P. Huestis (1977), Isostatic compensation on a continental scale; local versus regional mechanisms, *Geophysical Journal of the Royal Astronomical Society*, *51*(2), 431-452.

Banks, R. J., S. C. Francis, and R. G. Hipkin (2001), Effects of loads in the upper crust on estimates of the elastic thickness of the lithosphere, *Geophysical Journal International*, *145*(1), 291-299.

Beaumont, C. (1978), The evolution of sedimentary basins on a viscoelastic lithosphere; theory and examples, *Geophysical Journal Of The Royal Astronomical Society*, *55*(2), 471-497.

Beaumont, C. (1981), Foreland basins, *Geophysical Journal Of The Royal Astronomical Society*, *65*(2), 291-329.

Bird, P. (1984), Laramide crustal thickening event in the Rocky Mountain foreland and Great Plains, *Tectonics*, *3*(7), 741-758, doi:10.1029/TC003i007p00741.

Bird, P. (1988), Formation of the Rocky Mountains, Western United States; a continuum computer model, *Science*, *239*(4847), 1501-1507.

Bird, P. (1998), Kinematic history of the Laramide Orogeny in latitudes 35 degrees -49 degrees N, Western United States, *Tectonics*, *17*(5), 780-801, doi:10.1029/98TC02698.

Bloomfield, P. (2000), *Fourier analysis of time series. An introduction*, John Wiley & Sons, Inc., New York, United States.

Bradley, W. C. (1987), Erosion surfaces of the Colorado Front Range: a review, in *Geomorphic Systems of North America, Geological Society of America Centennial Special Volume, 2*, edited by W. L. Graf, pp. 215– 220, GSA, United States.

Brocher, T. M. (2005), Empirical Relations between Elastic Wavespeeds and Density in the Earth's crust, *SSA Bulletin*, *95*, 2081-2092, doi: 10.1785/0120050077.

Buffler, R. T. (2003), The Browns Park Formation in the Elkhead region, northwestern Colorado–south central Wyoming: Implications for Late Cenozoic sedimentation, in *Cenozoic systems of the Rocky Mountain region*, edited by R. G. Raynolds, and R. M. Flores, pp. 183-212, RMS for EPM, Denver, Colorado.

Burgess, P. M., M. Gurnis, and L. Moresi (1997), Formation of sequences in the cratonic interior of North America by interaction between mantle, eustatic, and stratigraphic processes, *Geological Society Of America Bulletin*, *109*(12), 1515-1535, doi:10.1130/0016-7606(1997)109<1515:FOSITC>2.3.CO;2.

Burov, E., C. Jaupart, and J. C. Mareschal (1998), Large-scale crustal heterogeneities and lithospheric strength in cratons, *Earth And Planetary Science Letters*, *164*(1-2), 205-219.

Chapin, C. E., and S. M. Cather (1994), Tectonic setting of the axial basins of the northern and central Rio Grande Rift, *Special Paper - Geological Society Of America*, *291*, 5-25.

Christensen, N. I., and W. D. Mooney (1995), Seismic velocity structure and composition of the continental crust; a global view, *Journal of Geophysical Research*, *100*(B6), 9761-9788, doi:10.1029/95JB00259.

Christiansen, R. L., and R. S. Yeats (1992), Chapter 7. Post-Laramide geology of the U.S. Cordilleran region, in *The Cordilleran Orogen, Conterminous U.S., The geology of North America, G-3*, edited by B. C. Burchfiel, P. W. Lipman, and M. L. Zoback, pp. 261–406, Geological Society of America, United States.

Cleary, J., and A. L. Hales (1966), An analysis of the travel times of P waves to North American stations, in the distance range 32 degrees to 100 degrees, *Bulletin of the Seismological Society of America*, *56*(2), 467-489.

Copland, J. R. (1984), Laramide structural deformation at the interface between the Laramie Range and the Denver-Julesburg Basin, Southeastern Wyoming, M.S. thesis, Dep. of Geol. and Geophys., Univ. of Wyoming, Laramie, Wyoming, USA.

Cross, T. A., and R. H. Jr. Pilger (1978), Tectonic controls of Late Cretaceous sedimentation, Western Interior, USA, *Nature* [London], *274*(5672), 653-657.

Curtis, B. F. (1975), Cenozoic History of the Southern Rocky Mountains, *Geol. Soc. Am. Mem.*, *144*, vii-viii.

DeCelles, P. G., M. B. Gray, K. D. Ridgway, R. B. Cole, P. Srivastava, N. Pequera, and D. A. Pivnik (1991), Kinematic history of a foreland uplift from Paleocene synorogenic conglomerate, Beartooth Range, Wyoming and Montana, *Geological Society Of America Bulletin*, *103*(11), 1458-1475, doi:10.1130/0016-7606(1991)103<1458:KHOAFU>2.3.CO;2.

Decker, E. R., K. R. Baker, G. R. Bucher, and H. P. Heasler (1980), Preliminary heat flow and radioactivity studies in Wyoming, *J. of Geophys. Res.*, *85*(B1), 311-321, doi:10.1029/JB085iB01p00311.

Decker, E. R., H. P. Heasler, K. L. Buelow, K. H. Baker, and J. S. Hallin (1988), Significance of past and recent heat-flow and radioactivity studies in the Southern Rocky Mountains region, *Geological Society of America Bulletin*, *100*(12), 1851-1885, doi:10.1130/0016-7606(1988)100<1851:SOPARH>2.3.CO;2.

Dickinson, W. R., and W. S. Snyder (1979), Geometry of subducted slabs related to San Andreas transform, *Journal Of Geology*, *87*(6), 609-627.

Dickinson, W. R, M. A. Klute, M. J. Hayes, S. U. Janecke, E. R. Lundin, M. A. McKittrick, and M. D. Olivares (1988), Paleogeographic and paleotectonic setting of Laramide sedimentary basins in the central Rocky Mountain region, *Geological Society of America Bulletin*, *100*, 1023-1039.

Dueker, K., H. Yuan, and B. Zurek (2001), Thick-structured Proterozoic lithosphere of the Rocky Mountain region, *GSA Today*, *11*(12), 4-9.

Eaton, G. P. (1987), Topography and origin of the southern Rocky Mountains and Alvarado Ridge, *Geological Society Special Publications*, *28*, 355-369.

Egan, S. S. (1992), The flexural isostatic response of the lithosphere to extensional tectonics, *Tectonophysics*, *202*(2-4), 291-308.

Egan, S. S., and J. M. Urquhart (1994), Numerical modelling of lithosphere shortening; application to the Laramide orogenic province, western USA, *Tectonophysics*, *221*, 385-411.

Epis, R. C, and C. E. Chapin (1974), Stratigraphic nomenclature of the Thirtynine Mile volcanic field, central Colorado, *U.S. Geological Survey Bulletin*, *1395-C*, C1-C23.

Epis, R. C, and C. E. Chapin (1975), Geomorphic and tectonic implications of the post-Laramide, late Eocene erosion surface in the southern Rocky Mountains, in *Cenozoic history of the southern Rocky Mountains*, *Geological Society of America Memoir*, vol. 144, edited by B. F. Curtis, pp. 45-74, GSA, Boulder, Colorado.

Forsyth, D. W. (1985), Subsurface loading and estimates of the flexural rigidity of continental lithosphere, *J. of Geophys. Res.*, *90*(12), 623-632.

Garner, D. L., and D. L. Turcotte (1984), The thermal and mechanical evolution of the Anadarko Basin, *Tectonophysics*, *107*(1-2), 1-24.

German, K. E. Jr. (1982), Secondary uranium enrichment of the Precambrian basement rock of Nebraska, M.S. thesis, Dep. of Geol., Univ. of Nebraska, Lincoln, Nebraska, USA.

Gilbert, H. (2012), Crustal structure and signatures of recent tectonism as influenced by ancient terranes in the western United States, *Geosphere*, *8*(1), 141–157, doi:10.1130/GES00720.1.

Gilbert, H. J., and A. F. Sheehan (2004), Images of crustal variations in the intermountain west, *Journal of Geophysical Research*, *109*(3), doi:10.1029/2003JB002730.

Goes, S., and S. van der Lee (2002), Thermal structure of the North American uppermost mantle inferred from seismic tomography, *Journal of Geophysical Research*, *107*(B3), doi:10.1029/2001JB000049.

Gries, R. (1983), North-south compression of Rocky Mountain foreland structures, in *Rocky Mountain Foreland Basins and Uplifts, Rocky Mountain Assoc. Geol. Field Conference Guidebook*, edited by J. D. Lowell, pp. 9-32, RMAG, Denver, Colorado.

Haxby, W. F., D. L. Turcotte, and J. M. Bird (1976), Thermal and mechanical evolution of the Michigan Basin, *Tectonophysics*, *36*(1-3), 57-75.

Heller, P. L., K. Dueker, and M. E. McMillan (2003), Post-Paleozoic alluvial gravel transport as evidence of continental tilting in the U.S. Cordillera, *Geological Society Of America Bulletin*, *115*(9), 1122-1132, doi:10.1130/B25219.1.

Hemborg, H. T. (1996), Basement structure map of Colorado with major oil and gas fields, *Colorado Geological Survey Map Series*, *30*, scale 1:1,000,000, Colorado Geological Survey, Denver, Colorado.

Henstock, T. J., and Deep Probe Working Group (1998), Probing the Archean and Proterozoic lithosphere of western North America, *GSA Today*, *8*(7), 1-5.

Higley, D. K., R. R. Charpentier, T. A. Cook, T. R. Klett, R. M. Pollastro, and J. W. Schmoker (2002), Executive summary – 2002; Assessment of undiscovered oil and gas in the Denver Basin province, Colorado, Kansas, Nebraska, South Dakota, and Wyoming, *U.S. Geological Survey Digital Data Series DDS–69–P*.

Holom, D. I., and J. S. Oldow (2007), Gravity reduction spreadsheet to calculate the Bouguer anomaly using standardized methods and constants, *Geosphere*, *3*(2), 86–90, doi: 10.1130/GES00060.1.

Hoy, R. G., and K. D. Ridgway (1997), Structural and sedimentological development of footwall growth synclines along an intraforeland uplift, east-central Bighorn Mountains, Wyoming, *Geological Society Of America Bulletin*, *109*(8), 915-935, doi:10.1130/0016-7606(1997)109<0915:SASDOF>2.3.CO;2.

Humphreys, E. D. (1995), Post-Laramide removal of the Farallon Slab, Western United States, *Geology* [Boulder], *23*(11), 987-990, doi:10.1130/0091-7613(1995)023<0987:PLROTF>2.3.CO;2.

Humphreys, E. D., and K. G. Dueker (1994), Physical state of the Western U.S. upper mantle, *Journal Of Geophysical Research*, *99*(B5), 9635-9650, doi:10.1029/93JB02640.

Humphreys, E., E. Hessler, K. Dueker, G. Farmer, E. Erslev, and T. Atwater (2003), How Laramide-age hydration of North American lithosphere by the Farallon Slab controlled subsequent activity in the Western United States, *International Geology Review*, *45*(7), 575-595.

Isaacson, L. B., and S. B. Smithson (1976), Gravity anomalies and granite emplacement in west-central Colorado, *Geological Society of America Bulletin*, *87*(1), 22-28.

Izett, G. A. (1975), Late Cenozoic sedimentation and deformation in northern Colorado and adjoining areas, *Memoir - Geological Society of America*, *144*, 179-209.

Jewett, J. M., and D. F. Merriam (1959), Geologic framework of Kansas; a review for geophysicists, *Bulletin - Kansas Geological Survey*, *137*, 9-52.

Johnson, R. A. (1985), Thrust faulting in the Laramie Mountains, Wyoming, from reanalysis of COCORP data, *Geology* [Boulder], *13*(8), 534-537.

Jordan, T. E. (1981), Thrust loads and foreland basin evolution, Cretaceous, Western United States, *Am. Assoc. Pet. Geol. Bull.*, *65*, 2506-2520.

Karlstrom, K. E., and CD-ROM Working Group (2002), Structure and evolution of the lithosphere beneath the Rocky Mountains; initial results from the CD-ROM experiment, *GSA Today*, *12*(3), 4-10.

Karlstrom, K. E., S. J. Whitmeyer, K. Dueker, M. L. Williams, S. A. Bowring, A. Levander, E. D. Humphreys, and G. R. Keller (2005), Synthesis of results from the CD-ROM experiment; 4-D image of the lithosphere beneath the Rocky Mountains and implications for understanding the evolution of continental lithosphere, in *The Rocky Mountain region; an evolving lithosphere; tectonics, geochemistry, and geophysics*, *Geophysical Monograph*, vol. 154, edited by K. E. Karlstrom, and G. R. Keller, pp. 421-441, AGU, Washington, D.C.

Karlstrom, K. E., R. Crow, L. J. Crossey, D. Coblentz, D., and J. W. van Wijk (2008), Model for tectonically driven incision of the younger than 6 Ma Grand Canyon, *Geology* [Boulder], *36*(11), 835-838, doi:10.1130/G25032A.1.

Karlstrom, K. E., and CREST Working Group (2011), Mantle-driven dynamic uplift of the Rocky Mountains and Colorado Plateau and its surface response; toward a unified hypothesis, *Lithosphere*, *4*(1), 3-22, doi:10.1130/L150.1.

Karner, G. D., and A. B. Watts (1983), Gravity anomalies and flexure of the lithosphere at mountain ranges, *J. Geophys. Res.*, *88*, 10449-10477.

Keefer, W. R., and J. D. Love (1963), Laramide vertical movements in central Wyoming, *Contributions To Geology*, *2*(1), 47-54.

Keller, R. G., C. M. Snelson, A. F. Sheehan, and K. G. Dueker (1998), Geophysical studies of crustal structure in the Rocky Mountain region; a review, *Rocky Mountain Geology*, *33*, issue 2, 217-228.

Keller, G. R., K. E. Karlstrom, M. L. Williams, K. C. Miller, C. Andronicos, A. Levander, C. Snelson, and C. Prodehl (2005), The dynamic nature of the continental crust-mantle boundary: Crustal evolution in the southern Rocky Mountain region as an example, in *The Rocky Mountain region; an evolving lithosphere; tectonics, geochemistry, and geophysics*, *Geophysical Monograph*, vol. 154, edited by K. E. Karlstrom, and G. R. Keller, pp. 403-420, AGU, Washington, D.C.

Kinney, D. M. (1967), Basement Map of North America, scale: 1:5,000,000, AAPG and USGS, Reston, Virginia.

Korenaga, J., and T. H. Jordan (2003), Physics of multiscale convection in Earth's mantle; onset of sublithospheric convection, *Journal of Geophysical Research*, *108*(B7), doi:10.1029/2002JB001760.

Lachenbruch, A. H., and J. H. Sass (1977), Heat flow in the United States and the thermal regime of the crust, *Geophysical Monograph*, *20*, 626-675.

Larson, S. M. (2009), Laramide transpression and oblique thrusting in the northeastern Front Range, Colorado; 3D kinematics of the Livermore Embayment, M.S. thesis, Dep. of Geosciences, Colorado State Univ., Fort Collins, Colorado, USA.

Lee, C. (2003), Compositional variation of density and seismic velocities in natural peridotites at STP conditions; implications for seismic imaging of compositional heterogeneities in the upper mantle, *Journal of Geophysical Research*, *108*(B9), doi:10.1029/2003JB002413.

Lee, D., and S. P. Grand (1996), Upper mantle shear structure beneath the Colorado Rocky Mountains, *Journal of Geophysical Research*, *101*(B10), 22,233-22,244, doi:10.1029/96JB01502.

Lerner-Lam, A. L., A. F. Sheehan, S. Grand, E. D. Humphreys, K. G. Dueker, E. Hessler, H. Guo, D.-K. Lee, and M. Savage (1998), Deep structure beneath the Southern Rocky Mountains from the Rocky Mountain Front broadband seismic experiment, *Rocky Mountain Geology*, *33*(2), 199-216.

Levander, A., C. Zelt, and M. Magnani (2005), Crust and upper mantle velocity structure of the Southern Rocky Mountains from the Jemez Lineament to the Cheyenne Belt, in *The Rocky Mountain region; an evolving lithosphere; tectonics, geochemistry, and geophysics*, *Geophysical Monograph*, vol. 154, edited by K. E. Karlstrom, and G. R. Keller, pp. 403-420, AGU, Washington, D.C.

Li, A., D. W. Forsyth, and K. M. Fischer (2002), Evidence for shallow isostatic compensation of the Southern Rocky Mountains from Rayleigh wave tomography, *Geology* [Boulder], *30*(8), 683-686, doi:10.1130/0091-7613(2002)030<0683:EFSICO>2.0.CO;2.

Lowell, J. D. (1983), Foreland deformation. Rocky Mountain Foreland Basins and Uplifts, in *Rocky Mountain Foreland Basins and Uplifts*, *Rocky Mountain Assoc. Geol. Field Conference Guidebook*, edited by J. D. Lowell, pp. 1-8, RMAG, Denver, Colorado.

Macario, A., A. Malinverno, and W. F. Haxby (1995), On the robustness of elastic thickness estimates obtained using the coherence method, *J. of Geophys. Res.*, *100*(B8), 15163-15172, doi:10.1029/95JB00980.

Mallory, W. W. (1972), *Geologic Atlas of the Rocky Mountain Region*, Rocky Mountain Assoc. Geol., Denver, Colorado.

McCoy, A. M., M. Roy, L. Trevino, and G. Keller (2005), Gravity modeling of the Colorado mineral belt, in *The Rocky Mountain region; an evolving lithosphere; tectonics, geochemistry, and geophysics*, *Geophysical Monograph*, vol. 154, edited by K. E. Karlstrom, and G. R. Keller, pp. 403-420, AGU, Washington, D.C.

McDonald, R. E. (1972), Eocene and Paleocene rocks of the southern and central basins, in *Geologic Atlas of the Rocky Mountain Region*, edited by W. W. Mallory, pp. 243-256, RMAG, Denver, Colorado.

McIntosh, W. C., and C. E. Chapin (1994), 40Ar/39Ar geochronology of ignimbrites in the Thirtynine Mile Volcanic Field, Colorado, in *Late Paleogene geology and paleoenvironments of Central Colorado, Geological Society of America Field Trip Guidebook*, edited by E. Evanoff, pp. 23–26, GSA, Boulder, Colorado.

McKenzie, D. (2003), Estimating T (sub e) in the presence of internal loads, *Journal of Geophysical Research*, *108*(B9), doi:10.1029/2002JB001766.

McKenzie, D., and D. Fairhead (1997), Estimates of the effective elastic thickness of the continental lithosphere from Bouguer and free air gravity anomalies, *Journal of Geophysical Research*, *102*, 27523-27552.

McMillan, M. E., P. L. Heller, and S. L. Wing (2006), History and causes of post-Laramide relief in the Rocky Mountain orogenic plateau, *Geological Society of America Bulletin*, *118*, 393–405, doi: 10.1130/B25712.1.

McQuarrie, N., and C. G. Chase (2000), Raising the Colorado Plateau, *Geology* [Boulder], *28*(1), 91-94, doi:10.1130/0091-7613(2000)028<0091:RTCP>2.3.CO;2.

Mooney, W. D., and M. K. Kaban (2010), The North American upper mantle: Density, composition, and evolution, *J. of Geophys. Res.*, *115*(B12), doi:10.1029/2010JB000866.

Morgan, P. P., and C. A. Swanberg (1985), On the Cenozoic uplift and tectonic stability of the Colorado Plateau, *Journal Of Geodynamics*, *3*(1-2), 39-63.

Morse, D. G. (1985), Oligocene paleogeography in the southern Denver Basin, in *Cenozoic paleogeography of the west-central United States*, edited by R. M. Flores and S. S. Kaplan, pp. 277-292, RMAG and SEPM, Denver, Colorado.

Moucha, R., A. M. Forte, D. B. Rowley, J. X. Mitrovica, N. A. Simmons, and S. P. Grand (2009), Deep mantle forces and the uplift of the Colorado Plateau, *Geophysical Research Letters*, 36(19), doi:10.1029/2009GL039778.

Naeser, C. W., B. Bryant, M. J. Kunk, K. S. Kellogg, R. A. Donelick, W. J. Jr. Perry (2002), Tertiary cooling and tectonic history of the White River Uplift, Gore Range, and western Front Range, central Colorado; evidence from fission-track and (super 39) Ar/ (super 40) Ar ages, *Special Paper - Geological Society Of America*, *366*, 31-53.

Olsen, K. H., G. R. Keller, and J. N. Stewart (1979), Crustal structure along the Rio Grande Rift from seismic refraction profiles, in *Rio Grande Rift: Tectonics and Magmatism*, *Am. Geophys. Union Monograph*, edited by R. E. Riecker, pp. 127-144, AGU, Washington, D.C.

Parker, R. L. (1972), The rapid calculation of potential anomalies, *Geophysical Journal of the Royal Astronomical Society*, *31*(4), 447-455.

Petit, C., and C. Ebinger (2000), Flexure and mechanical behavior of cratonic lithosphere; gravity models of the East African and Baikal rifts, *Journal of Geophysical Research*, *105*(B8), 19. doi:10.1029/2000JB900101.

Porath, H. H. (1971), Magnetic variation anomalies and seismic low-velocity zone in the western United States, *J. of Geophys. Res.*, *76*(11), 2643-2648.

Raynolds, R. G. (2002), Upper Cretaceous and Tertiary stratigraphy of the Denver Basin, Colorado, *Rocky Mountain Geology*, *37*, 111-134.

Raynolds, R. G., K. R. Johnson, B. Ellis, M. Dechesne, and I. M. Miller (2007), Earth history along Colorado's Front Range; salvaging geologic data in the suburbs and sharing it with the citizens, *GSA Today*, *17*(12), 4-10, doi:10.1130/GSATO1712A.1.

Reinke, R. F. (1991), Three-dimensional gravity and flexural analysis of the Denver Basin, the Great Plains, and adjacent basement uplifts, M.S. thesis, Dep. of Geol. and Geophys., Univ. of Wyoming, Laramie, Wyoming, USA.

Roy, M., K. Karlstrom, S. Kelley, F. J. Pazzaglia, and S. Cather (1999), Topographic setting of the Rio Grande Rift, New Mexico: Assessing the role of flexural "rift-flank uplift" in the Sandia Mountains, *New Mexico Geological Society Guidebook, 50,* p. 167–174.

Royden, L., and G. D. Karner (1984), Flexure of lithosphere beneath Apennine and Carpathian foredeep basins; evidence for an insufficient topographic load, *AAPG Bulletin*, *68*(6), 704-712, doi:10.1306/AD461372-16F7-11D7-8645000102C1865D.

Rumpfhuber, E.-M., and R. G. Keller (2009), An integrated analysis of controlled and passive source seismic data across an Archean-Proterozoic suture zone in the Rocky Mountains, *J. of Geophys. Res.*, *114*, B08305, doi:10.1029/2008JB005886.

Sakamaki, T., E. Ohtani, S. Urakawa, H. Terasaki, and Y. Katayama (2011), Density of carbonated peridotite magma at high pressure using an X-ray absorption method, *American Mineralogist*, *96*(4), 553-557, doi:10.2138/am.2011.3577.

Schmandt, B., and E. Humphreys (2010), Complex subduction and small-scale convection revealed by body-wave tomography of the Western United States upper mantle, *Earth and Planetary Science Letters*, *297*(3-4), 435-445, doi:10.1016/j.epsl.2010.06.047.

Schott, B., D. A. Yuen, and H. Schmeling (2000), The diversity of tectonics from fluid-dynamical modeling of the lithosphere-mantle system, *Tectonophysics*, *322*(1-2), 35-51.

Scott, G. R. (1975), Cenozoic surfaces and deposits in the southern Rocky Mountains, *Geological Society of America Memoir 144*, 227–248.

Severinghaus, J., and T. Atwater (1990), Cenozoic geometry and thermal state of the subducting slabs beneath western North America, *Memoir - Geological Society Of America*, *176*, 1-22.

Sheehan, A. F., G. A. Abets, C. H. Jones, and A. L. Lerner-Lam (1995), Crustal thickness variations across the Colorado Rocky Mountains from teleseismic receiver functions, *J. of Geophys. Res.*, *100*(B10), 20391-20404.

Simons, F. J., M. T. Zuber, and J. Korenaga (2000), Isostatic response of the Australian lithosphere; estimation of effective elastic thickness and anisotropy using multitaper spectral

analysis, *Journal of Geophysical Research*, *105*(B8), 19,163-19,184, doi:10.1029/2000JB900157.

Snelson, C. M., T. J. Henstock, G. R. Keller, K. C. Miller, and A. R. Levander (1998), Crustal and uppermost mantle structure along the Deep Probe seismic profile, *Rocky Mt. Geol.*, *33*, 181-198.

Snelson, C. M., G. Keller, K .C. Miller, H. Rumpel, and C. Prodehl (2005), Regional crustal structure derived from the CD-ROM 99 seismic refraction/wide-angle reflection profile; the lower crust and upper mantle, in *The Rocky Mountain region; an evolving lithosphere; tectonics, geochemistry, and geophysics*, *Geophysical Monograph*, vol. 154, edited by K. E. Karlstrom, and G. R. Keller, pp. 403-420, AGU, Washington, D.C.

Spencer, J. E. (1996), Uplift of the Colorado Plateau due to lithosphere attenuation during Laramide low-angle subduction, *Journal of Geophysical Research*, *101*(B6), 13,595-13,609, doi:10.1029/96JB00818.

Stanley, K. O., and W. J. Wayne (1972), Epeirogenic and Climatic Controls of Early Pleistocene Fluvial Sediment Dispersal in Nebraska, *Geological Society of America Bulletin*, *83*(12), 3675-3690, doi:10.1130/0016-7606(1972)83[3675:EACCOE]2.0.CO;2.

Steidtmann J. R., and L. T. Middleton (1991), Fault chronology and uplift history of the southern Wind River Range, Wyoming; implications for Laramide and post-Laramide deformation in the Rocky Mountain foreland, *Geological Society of America Bulletin*, *103*(4), 472-485.

Stewart, J., and A. B. Watts (1997), Gravity anomalies and spatial variations of flexural rigidity at mountain ranges, *Journal of Geophysical Research*, *102*(B3), 5327-5253. doi:10.1029/96JB03664.

Trimble, D. E. (1980), Cenozoic tectonic history of the Great Plains contrasted with that of the southern Rocky Mountains: a synthesis, *Mountain Geologist*, *17*(3), 59-69.

Turcotte, D. L., and G. Schubert (2002), *Geodynamics*, Cambridge University Press, Cambridge, United Kingdom.

Tweto, O. O. (1975), Laramide (late Cretaceous-early Tertiary) orogeny in the southern Rocky Mountains, *Memoir - Geological Society of America, 144*, 1-44.

Tweto, O. O. (1979a), The Rio Grande rift in Colorado, in *Rio Grande Rift: Tectonics and Magmatism*, *Am. Geophys. Union Monograph*, edited by R. E. Rieker, pp. 33-56, AGU, Washington, D.C.

Tweto, O. O. (1979b), Geologic map of Colorado, scale 1:500,000, USGS, Reston, Virginia.

Tweto, O. O. (1980), Tectonic history of Colorado, in *Colorado Geology, Rocky Mountain Association of Geologists Field Conference Guidebook*, edited by H. C. Kent, and K. W. Porter, pp. 5-9.

Van Wijk, J. W., W. S. Baldridge, J. van Hunen, S. Goes, R. Aster, D. D. Coblentz, S. P. Grand, and J. Ni (2010), Small-scale convection at the edge of the Colorado Plateau; implications for topography, magmatism, and evolution of Proterozoic lithosphere, *Geology* [Boulder], *38*(7), 611-614, doi:10.1130/G31031.1.

Walcott, R. I. (1970), Flexural rigidity, thickness, and viscosity of the lithosphere, *Journal of Geophysical Research*, *75*(20), 3941-3954.

Watkins, J. S. (1964), Basement depths from widely spaced aeromagnetic profiles in Kansas and Nebraska, *Geophysics*, *29*, 80-86.

Watts, A. B., G. D. Karner, and M. S. Steckler (1982), Lithospheric flexure and the evolution of sedimentary basins, *Philosophical Transactions Of The Royal Society Of London, Series A: Mathematical And Physical Sciences*, *305*(1489), 249-281.

Weimer, R. J. and S. A. Sonnenberg (1996), Guide to the petroleum geology and Laramide orogeny, Denver Basin and Front Range, Colorado, *Colorado Geological Survey Bulletin, 51*.

APPENDIX

Table A1. Well data taken from the COGCC database (cogcc.co.us). Values for each formation represent elevation in meters (negative for above sea level)

Well API Number	Latitude	Longitude	Precambrian (m)	Niobrara (m)	Pierre (m)	Fox Hills (m)	Laramie (m)
			North Profile				
05-095-06047	40.645	-102.178		-396			
05-095-06022	40.633	-102.180		-394			
05-095-05080	40.631	-102.203	672	-402			
05-095-06009	40.635	-102.275		-367			
05-095-06001	40.638	-102.337		-321			
05-095-06043	40.633	-102.410		-368			
05-095-06068	40.632	-102.425		-373			
05-095-06006	40.648	-102.663		-317			
05-075-05776	40.655	-102.696		-412			
05-075-05697	40.644	-102.907		-231			
05-075-08967	40.648	-102.930		-223			
05-075-08347	40.655	-102.936		-237			
05-075-08891	40.654	-102.937		-237			
05-075-08949	40.649	-102.937		-218			
05-075-08968	40.641	-102.941		-218			
05-075-08966	40.648	-102.946		-228			
05-075-05708	40.647	-102.978		-214			
05-075-05767	40.655	-102.989		-216			
05-075-07461	40.633	-102.994		-207			
05-075-08630	40.651	-102.996		-217			
05-075-07460	40.643	-102.997		-205			
05-075-05765	40.655	-102.999		-211			
05-075-07459	40.651	-102.999		-216			
05-075-05736	40.652	-103.003		-192			
05-075-05715	40.648	-103.005		-208			
05-075-05650	40.633	-103.012		-204			
05-075-08187	40.644	-103.022		-203			
05-075-08723	40.643	-103.023		-208			
05-075-08586	40.651	-103.023		-206			
05-075-05759	40.655	-103.028		-194			
05-075-05627	40.628	-103.029		-199			
05-075-08752	40.644	-103.032		-213			
05-075-08673	40.638	-103.035		-204			
05-075-08587	40.643	-103.037		-187			
05-075-08568	40.654	-103.047		-205			
05-075-08883	40.654	-103.052		-201			
05-075-05723	40.650	-103.071		-185			
05-075-08946	40.645	-103.099		-169			
05-075-08095	40.643	-103.099		-169			

05-075-08655	40.636	-103.099	-145	
05-075-05764	40.655	-103.105	-174	
05-075-05623	40.628	-103.107	-149	
05-075-08945	40.631	-103.109	-169	
05-075-08118	40.638	-103.111	-165	
05-075-05762	40.655	-103.118	-163	
05-075-60010	40.647	-103.119	-162	
05-075-08829	40.650	-103.124	-171	
05-075-08524	40.632	-103.138	-160	
05-075-08986	40.650	-103.157	-163	
05-075-08105	40.635	-103.176	-139	
05-075-08221	40.653	-103.219	-108	
05-075-08190	40.645	-103.224	-116	
05-075-09246	40.645	-103.233	-98	
05-075-08216	40.641	-103.243	-104	
05-075-05726	40.650	-103.274	-84	
05-075-05687	40.640	-103.294	-74	
05-075-05671	40.637	-103.332	-48	
05-075-08375	40.642	-103.342	-50	
05-075-05689	40.640	-103.370	-53	
05-075-08497	40.640	-103.380	-35	
05-075-05673	40.637	-103.384	-33	-1296
05-075-05679	40.638	-103.402	-19	-1008
05-075-08172	40.634	-103.426	0	
05-075-05684	40.640	-103.432	-4	
05-075-05680	40.638	-103.459	20	
05-075-05664	40.634	-103.478	21	
05-075-09033	40.641	-103.541	53	
05-075-05690	40.641	-103.550	65	
05-075-08315	40.638	-103.565	101	
05-123-07167	40.645	-103.593	88	
05-123-09353	40.641	-103.617	101	
05-123-06148	40.634	-103.627	107	
05-123-07107	40.644	-103.650	135	
05-123-11867	40.649	-103.660	124	
05-123-06117	40.626	-103.708	145	
05-123-13702	40.641	-103.741	185	
05-123-08309	40.646	-103.809	226	
05-123-11095	40.642	-103.837	247	
05-123-10795	40.638	-103.852	244	
05-123-13276	40.642	-103.870	267	
05-123-14267	40.642	-103.880	262	
05-123-13619	40.634	-103.904	286	
05-123-14126	40.634	-103.928	289	
05-123-08043	40.631	-103.966	311	
05-123-05548	40.646	-103.990	326	

05-123-19932	40.639	-103.997		331			
05-123-08598	40.639	-104.028		347			
05-123-05511	40.635	-104.037		347			
05-123-14414	40.643	-104.056		362			
05-123-08700	40.642	-104.080		370			
05-123-11180	40.642	-104.090		377			
05-123-09375	40.642	-104.123		384			
05-123-19448	40.629	-104.128		380			
05-123-07125	40.631	-104.161		395			
05-123-10939	40.631	-104.218		437			
05-123-05506	40.631	-104.223		442			
05-123-10402	40.641	-104.242		444	-1354	-1439	
05-123-08167	40.649	-104.261		467			
05-123-07721	40.641	-104.409		544			
05-123-12335	40.637	-104.489		540			
05-123-11951	40.630	-104.523		588			
05-123-12266	40.627	-104.542		576			
05-123-12085	40.629	-104.566		598			
05-123-12262	40.640	-104.599		624			
05-123-12337	40.625	-104.604		619			
05-123-12336	40.640	-104.623		631			
05-123-10188	40.626	-104.646		652			
05-123-09855	40.648	-104.713		671	-1309		
05-123-05536	40.649	-104.718		672			
05-123-05525	40.642	-104.747		621			
05-123-07011	40.638	-104.761		611			
05-123-05502	40.628	-104.775		621			
05-123-05522	40.642	-104.809		527			
05-123-09054	40.643	-104.826		0	-1480		
05-123-11778	40.638	-104.862		550			
05-123-08834	40.626	-104.924		501			
05-069-06111	40.641	-104.979		347			
05-069-06072	40.641	-105.007		142			
05-069-06083	40.641	-105.036		-251			
05-069-05114	40.641	-105.051	660	-453			
05-069-06279	40.638	-105.118		-1248			
05-057-06154	40.640	-106.098		-301			
05-057-06110	40.638	-106.106		-275	-2052		
05-057-06071	40.644	-106.314		717			-836
Central Profile							
05-125-07089	39.706	-102.053		-649			
05-125-10604	39.705	-102.071		-686			
05-125-11212	39.707	-102.097		-665			
05-125-06461	39.702	-102.127		-652			
05-125-08832	39.710	-102.145		-661	-1071		

05-125-08681	39.696	-102.167	-672	-1081
05-125-08349	39.704	-102.185	-682	-1084
05-125-07678	39.702	-102.200	-689	
05-125-08399	39.703	-102.234	-704	-1095
05-125-06778	39.705	-102.247	-693	-1097
05-125-07886	39.701	-102.255	-701	
05-125-06893	39.697	-102.284	-678	-1106
05-125-08742	39.692	-102.314	-698	
05-125-06494	39.697	-102.693	-634	
05-121-05093	39.690	-102.857	-605	
05-121-08522	39.694	-102.866	-599	
05-121-05114	39.701	-102.880	-544	
05-121-08928	39.708	-102.923	-585	
05-121-08860	39.709	-102.967	-569	
05-121-05113	39.701	-102.980	-552	
05-121-08589	39.704	-103.008	-542	
05-121-10513	39.701	-103.026	-547	
05-121-05147	39.711	-103.030	-548	
05-121-05112	39.701	-103.078	-541	
05-121-08168	39.693	-103.092	-547	
05-121-09211	39.693	-103.172	-507	
05-121-07619	39.700	-103.191	-497	
05-121-08472	39.696	-103.211	-494	
05-121-07705	39.699	-103.225	-489	
05-121-08669	39.695	-103.243	-470	
05-121-09419	39.702	-103.267	-444	
05-121-09253	39.706	-103.281	-453	
05-121-05144	39.709	-103.300	-440	
05-121-09290	39.694	-103.328	-404	
05-121-05117	39.701	-103.347	-425	
05-121-10014	39.702	-103.357	-430	
05-121-09367	39.707	-103.371	-415	
05-121-08602	39.708	-103.404	-397	
05-121-05105	39.694	-103.410	-393	
05-121-08078	39.701	-103.432	-386	
05-121-07709	39.701	-103.456	-379	
05-121-09696	39.698	-103.474	-365	
05-121-08630	39.705	-103.493	-337	
05-121-07637	39.698	-103.512	-341	
05-121-08890	39.705	-103.526	-332	
05-121-08590	39.691	-103.540	-325	
05-121-05146	39.709	-103.559	-305	
05-121-10430	39.713	-103.587	-273	
05-121-08154	39.709	-103.600	-282	
05-121-09674	39.698	-103.615	-270	
05-121-05130	39.705	-103.638	-251	

05-121-08888	39.698	-103.662	-238		
05-121-08158	39.705	-103.676	-227		
05-121-08144	39.698	-103.695	-219		
05-005-06206	39.713	-103.723	-192		
05-005-05044	39.684	-103.742	-184		
05-005-06717	39.705	-103.759	-172		
05-005-06768	39.704	-103.766	-182		
05-005-06076	39.698	-103.786	-162		
05-005-06945	39.702	-103.804	0		
05-005-06875	39.706	-103.859	-89		
05-005-07002	39.706	-103.878	-62		
05-005-06075	39.699	-103.926	-6		
05-005-05053	39.712	-103.964	20		
05-005-06267	39.710	-103.982	35		
05-005-06438	39.705	-103.990	31		
05-005-06761	39.702	-104.021	41	-1491	
05-005-06771	39.705	-104.029	59		
05-005-06351	39.694	-104.056	71		
05-005-06261	39.706	-104.067	97		
05-005-06130	39.706	-104.082	102		
05-005-06258	39.699	-104.112	150		
05-005-06601	39.712	-104.119	136		
05-005-06231	39.694	-104.136	151		
05-005-06183	39.698	-104.156	162		
05-005-06394	39.707	-104.185	209		
05-005-06666	39.697	-104.193	209		
05-005-06566	39.701	-104.217	232		
05-005-06126	39.701	-104.240	252		
05-005-06847	39.693	-104.273	427		
05-005-06929	39.704	-104.296	300		
05-005-06893	39.701	-104.315	315		-1355
05-005-06433	39.704	-104.338	334		
05-005-06667	39.697	-104.343	330		
05-005-06511	39.697	-104.376	357		
05-005-06784	39.707	-104.399	385		
05-005-06408	39.700	-104.418	399		-1260
05-005-06380	39.707	-104.450	425		
05-005-06504	39.711	-104.469	454		
05-005-06796	39.696	-104.483	444		-1272
05-005-06377	39.696	-104.492	465		
05-005-06830	39.712	-104.525	496		-1243
05-005-06523	39.697	-104.539	490		-1242

05-005-06858	39.698	-104.548		514	-1241
05-005-06554	39.698	-104.662		634	-1100
05-005-06500	39.709	-104.676		632	
			South Profile		
05-011-06017	38.058	-103.048	659		
05-089-06007	38.046	-104.016	657		
05-101-05020	38.043	-104.943	-1198		

CHAPTER 3

SUMMARY AND RECOMMENDATIONS

3.1 Summary

The objectives of this project are to estimate the location and magnitude of the load required to produce the current subsidence of the Denver Basin and construct three regional lithosphere-scale cross-sections to understand the total load distribution between the current topography and the subsurface. The cross-sections are constructed through flexural modeling of the shape of the Denver Basin and by spectral analysis and forward gravity modeling.

Average layered density models along each profile were obtained from the Bouguer gravity spectra analysis for each of the three gravity profiles in the north, central and south parts of the Denver Basin. The analysis revealed 5-6 linear segments in the logarithmic power spectra corresponding to subsurface density interfaces, three of which were further used in the flexural modeling. The interfaces are interpreted to represent the lithospheric thickness, at average depths of 132 to 153 km, base of the crust (45-55 km), mid-crustal boundary (about 20 km), average Precambrian basement depth (1-2 km), and boundary between Pierre Shale and "MzPz" layers (-1-0 km).

Flexural modeling of the depth to the basement unconformity in the Denver Basin, as constrained by the well data (German, 1982; cogcc.state.co.us: Chapter 2, Table A1) and Precambrian basement maps for Colorado, Kansas, and Nebraska (Jewett and Merriam, 1959; Watkins, 1964; Hemborg, 1996), requires a load magnitude of 2-5 x 10^{12} N/m and elastic thickness of 58-80 km of the lithosphere in the study area. The Bouguer gravity anomaly produced by the basement flexure of the Denver basin is much less than what is observed (Chapter 2, Figure 9). The large gravity low cannot be explained without a large subsurface mass deficit.

Consequently, four families of gravity models were produced for each profile to examine the position of the required buoyant subsurface load: (1) a family of models in which the requisite buoyant load is located entirely within the asthenosphere, (2) a family of models in which the buoyant load is placed entirely within the lithospheric mantle, (3) a family of models in which all the requisite load is in the lower crust, and (4) a family of models with the buoyant load located only in the upper crust. Densities required to produce the necessary mass deficiency are low compared to global average densities of lithosphere mantle and crust rocks in models in which the load is entirely within the lithosphere. The densities required to place the required buoyant load entirely within a given depth interval are: lithospheric mantle – 3.1-3.16 g/cc; lower crust – 2.76-2.89 g/cc; upper crust – 2.63-2.7 g/cc. The asthenosphere family of models is unable to simultaneously fit the magnitude and the wavelength of the gravity anomaly. These results imply some combination of the load partitioning between different depth levels beneath the Rocky Mountain Front Range.

3.2 Recommendations

To entirely understand the complexity of the tectonic evolution of the Denver Basin much more research and field data are necessary. Recommendations for future projects that could cast more light on the processes controlling the evolution of the basin, and also to improve collecting gravity data and modeling procedures include:

1. The data coverage of the gravity data together was quite good along the profiles, but was not dense enough in the regions adjacent to the profiles to apply additional analysis techniques, such as admittance and coherence analysis of the gravity and topography signals, that require a two-dimensional distribution of data. It is recommended to collect more gravity and topography data in the required profile vicinity for such analyses.

2. It would be useful to collect more gravity data in the mountain regions, because it would diminish the topographic effect of the frequent elevation fluctuation in the western part of the profiles.
3. One of the important factors in making corrections for the gravity data is measuring an elevation at the gravity stations as precisely as possible. In the present survey the elevation was measured with a handheld GPS receiver with a 30 m accuracy for the purposes of locating the station position, but the elevation used for the free air and Bouguer gravity corrections was taken from the digital USA topographic map with a 10 m accuracy. This did not affect the estimated Bouguer gravity value at the station too much (it caused the magnitude of uncertainty to be ±3 mGal). However, it's recommended to use a differential GPS system in further gravity surveys in the study area to improve the gravity uncertainty by at least an order of magnitude.
4. It's advisable to try using inverse flexural modeling for the same gravity dataset to gain a more robust quantitative understanding of the uncertainties involved in the parameter estimates. A joint inversion scheme that permits variability in elastic thickness, load value, position of the load, and considers load of current topography and well data, allowing for realistic geological conditions, would improve the potential of using flexural modeling to evaluate basin subsidence.
5. Because both the shape of the basin and the way in which the subsurface load is partitioned change along strike, it would also be useful to construct a 3D flexural model of the basin subsidence, or at least build more gravity and flexural models perpendicular to the basin axis.
6. The methods used in this thesis are portable. A similar workflow should be useful in other foreland basin areas.

REFERENCES

German, K. E. Jr. (1982), Secondary uranium enrichment of the Precambrian basement rock of Nebraska, M.S. thesis, Dep. of Geol., Univ. of Nebraska, Lincoln, Nebraska, USA.

Hemborg, H. T. (1996), Basement structure map of Colorado with major oil and gas fields, *Colorado Geological Survey Map Series*, *30*, scale 1:1,000,000, Colorado Geological Survey, Denver, Colorado.

Jewett, J. M., and D. F. Merriam (1959), Geologic framework of Kansas; a review for geophysicists, *Bulletin - Kansas Geological Survey*, *137*, 9-52.

Watkins, J. S. (1964), Basement depths from widely spaced aeromagnetic profiles in Kansas and Nebraska, *Geophysics*, *29*, 80-86.